UNCLASSIFIED

AAEC/E99

AAEC/E99

AUSTRALIAN ATOMIC ENERGY COMMISSION

RESEARCH ESTABLISHMENT

LUCAS HEIGHTS

THE EFFECT OF NEUTRON IRRADIATION ON BERYLLIUM OXIDE

by

B. S. HICKMAN

Issued Sydney, October 1962

UNCLASSIFIED

AUSTRALIAN ATOMIC ENERGY COMMISSION

RESEARCH ESTABLISHMENT

LUCAS HEIGHTS

THE EFFECT OF NEUTRON IRRADIATION ON BERYLLIUM OXIDE

by

B. S. HICKMAN

ABSTRACT

Fast neutron irradiation affects the properties of beryllium oxide by causing displacements and by causing nuclear transmutations. This report outlines the overall aims of a programme to investigate this problem, reviews the information from overseas laboratories, and describes the results obtained to date at Lucas Heights.

Results are given of measurements of properties of beryllium oxide fabricated by various methods and irradiated to doses of up to 7×10^{20} nvt (fission neutrons) at temperatures of 75 – 700 °C. The properties include macroexamination, dimensions, porosity, lattice parameter and line broadening, mechanical properties, thermal conductivity, metallography, and long wavelength neutron scattering. It is shown that an anisotropic lattice growth occurs which results in crumbling of the material at high doses. The damage rate is much smaller for irradiation at 500 – 700 °C than for equivalent doses at 100 °C. Fine-grained ($<3\mu$) material withstands crumbling up to much higher doses than coarse-grained material. The relationship between macroscopic growth, lattice growth, and the cracking and powdering is discussed in some detail and the results used to show the reasons for apparent discrepancies in data from overseas laboratories. Information relating to the defect structure is discussed and it is suggested that interstitial clusters in the basal planes are probably the cause of the marked anisotropy in the lattice growth. The effect of neutron energy spectrum on the damage rate is discussed and finally the potential of beryllium oxide as a reactor material is assessed.

It is concluded that very fine grained material should withstand doses of at least $1 - 2 \times 10^{21}$ nvt at temperatures of 500 – 1000 °C without serious deterioration of properties. More information, particularly on changes of mechanical properties and thermal conductivity, is required to confirm this conclusion and to ascertain whether the material will withstand higher doses.

CONTENTS

(continued)

CONTENTS (continued)

1. INTRODUCTION

Beryllium oxide is under consideration as a moderator and fuel dispersant for the Australian Atomic Energy Commission high temperature gas–cooled reactor project.

Investigations of the effect of neutron irradiation on beryllium oxide have been in progress at Lucas Heights for some time and some aspects of the work have already been published. Other work is being prepared for publication. At the time the investigations began little information on the subject was available from overseas laboratories, but recently some information has become available. Therefore an attempt is made to assess the present state of knowledge on the subject in this report. The problem and the aims of the Lucas Heights programme are stated briefly, information available from overseas is reviewed, and all the results obtained to date at Lucas Heights are discussed.

There are two mechanisms by which neutron irradiation can affect the properties of beryllium oxide. First, fast neutrons can cause displacements of atoms from their normal lattice positions, resulting in the formation of interstitial atoms and vacancies. These defects will disturb the regularity of the lattice and hence affect any properties which are dependent on this regularity. The defects may diffuse and recombine at elevated temperatures but since beryllium oxide has a high melting point, annealing may not occur until quite high temperatures are reached. The second mechanism is the fast neutron transmutation reactions which result in the formation of helium and tritium. These reactions are:

(i) $^{9}Be\ (n,2n)\ 2^{4}He$ which has a neutron energy threshold of 1.85 MeV.

(ii) $^{9}Be\ (n,\alpha)\ ^{6}He \xrightarrow{\beta-} {}^{6}Li$ which has a threshold of about 0.71 MeV.

The Li–6 formed in the second reaction is partly transformed to helium and tritium by thermal neutron capture. The net effect of these reactions is to produce an atomic dispersion of helium and tritium in the lattice. At low temperatures these atoms will remain in enforced solid solution but at elevated temperatures diffusion may occur and the gas will collect into bubbles which will cause volume increases and affect the properties.

In the H.T.G.C. breeder reactor concept based on beryllium oxide, under study at Lucas Heights, the fuel element will probably consist of a dispersion of uranium and thorium oxide in beryllium oxide. The overall uranium to beryllium atom ratios which have been considered vary from 1:250 up to 1:10,000. The concept of dispersion type fuel elements as applied to this system was discussed in detail by Hickman (1962); it was shown that provided a coarse fuel particle size is used and that the volume per cent. of dispersed phase is less than 25 – 30 per cent., the damage from fission products will be limited to the fuel particles and the region immediately surrounding them. The majority of the beryllium oxide matrix will then remain undamaged by fission products. The behaviour of the matrix under fast neutron irradiation will therefore be the main factor determining the fuel element life.

A. Abrahart (unpublished) has shown that for the fuel ratings (1–3 MW/Kg) and compositions under consideration, approximately 0.6 atoms of helium will be produced for each uranium atom consumed. Using this information, the helium concentrations and the integrated fission neutron doses for a burn–up of 100 per cent. (which is the minimum likely to give an economical system) and for a burn–up of 300 per cent., were calculated for various uranium–beryllium atom ratios. The results are given in Table 1.

NOTE: Burn–up is here defined as the percentage ratio of the number of fissions to the number of uranium atoms originally present.

It can be seen that fast neutron doses of the order of 10^{21} nvt will be sustained by the beryllium oxide matrix for the compositions of most interest (U:Be ratio from 1:1000 to 1:2000). Any fixed beryllium oxide moderator would be required to withstand doses of about 10^{22} nvt over the life of a reactor.

The two main aims of the research programme at Lucas Heights on irradiation effects in beryllium oxide are:

(i) To determine the effect of neutron irradiation on those properties of beryllium oxide of significance in reactor design and the effect of fabrication and structural variables on changes of properties, the ultimate aim being to specify the limits of temperature, neutron dose, stress, etc., within which the material can be satisfactorily used.

(ii) To gain an understanding of the mechanisms which produce the observed changes of properties.

An understanding of the mechanisms involved is essential for proper assessment of the results of property changes, to enable extrapolation of these results to different conditions, and to open up the possibility of developing material with greater resistance to detrimental property changes. Hence the two aims are closely integrated in the experimental programme.

The effects of the following variables on the changes of properties are being investigated:

- Fabrication method and hence density, grain size, degree of preferred orientation, etc.
- Additions of other materials such as Al_2O_3, MgO, CaO.
- Irradiation temperature.
- Irradiation dose.

The following post-irradiation measurements are being made:

- Density and dimensions.
- Mechanical properties including modulus of rupture, compressive strength, and elastic modulus.
- Microstructure using both optical and electron microscopy.
- X-ray lattice parameters and line broadening.
- Thermal conductivity.
- Stored energy.
- Long wavelength neutron scattering.
- Electrical resistivity.

Specimens in the various sizes required for the above measurements have been, or will be irradiated at either pile temperatures (75 – 100 °C) or at elevated temperatures (300 – 1200 °C). Although the pile temperature irradiation is not directly relevant to reactor technology, a faster damage rate can be obtained at these temperatures and studies of behaviour on annealing at elevated temperatures can provide much useful information. As these irradiations are much simpler than the high temperature irradiations, they are used extensively in the programme.

Because hot pressing was the first fabrication method developed at Lucas Heights, all the early work was done on high density hot-pressed material. More recently, irradiation of both hot-pressed and cold-pressed and sintered material of various grain sizes and densities has been done. Detailed description of much of the work on individual property measurements will be found in existing or future publications.

It must be emphasised that the Lucas Heights programme is still in its early stages and much more information is required both from in-pile and out-of-pile investigations before confident predictions can be made of the behaviour of beryllium oxide in a reactor environment at high temperatures and high doses. However the information obtained so far, combined with that obtained from overseas laboratories, enables some predictions to be made.

Further summary reports will be issued as more information becomes available.

2. REVIEW OF LITERATURE

Clarke (1962) recently reviewed all the information on irradiation damage in beryllium oxide which was available up to the end of 1961, including some unpublished information. In the following sections the available information about various property changes is reviewed including data made available since Clarke's review. The primary sources of the information were as follows:

Oak Ridge National Laboratory	– Shields, Lee, and Browning (1962)
General Atomic, San Diego	– Tobin (1962)
A.E.R.E., Harwell	– Clarke, Tappin, and Ghosh (1961)
	– Clarke (1962)
C.E.A., Saclay	– Elston and Caillat (1958)
	– Elston and Labbe (1961)
	– Elston (1962)
General Electric Laboratories, Evandale	– Unpublished information referred to by Clarke (1962)

2.1 Powdering and Cracking

Several workers observed cracking and powdering in irradiated beryllium oxide, (Shields et al. 1962, Tobin 1962, and Elston and Caillat 1958). Clarke (1962) reviewed the available information on these phenomena and concluded that:

(i) Powdering and cracking are two distinct phenomena, the latter being associated with thermal stress effects.

(ii) There is little correlation between the results of various workers on the dose and temperature required to cause powdering. However, it occurs more readily for high doses at low temperatures.

The results are very confusing. For instance Shields et al. (1962) reported that, of two nominally identical specimens irradiated under the same conditions, one powdered and the other was apparently unaffected. They suggested that either defect production or helium production could have caused the powdering although their reasons for the latter conclusion are difficult to follow. Elston and Labbe (1961) also suggested that powdering could have been due to either mechanism but, more recently, Elston (1962) stated that the powdering was due to the anisotropic growth process resulting from lattice defects.

The Lucas Heights work published earlier (Sabine et al. 1962), and the work described in Section 5.1 of this report shows conclusively that crumbling is due to the anisotropic growth process and explains the apparent discrepancies in overseas work.

2.2 Macroscopic Growth

Most workers have reported macroscopic growth and the results were examined by Clarke (1962). He concluded that they indicate that:

(i) Growth is approximately linear with dose and the results of most workers are in general agreement.

(ii) The growth in high density materials is greater than in low density materials.

(iii) The theoretical growth at low doses is intermediate between the growth of high and low density material. Elston and Labbe (1961) suggested that this is due to cracking and growth of voids in the high density material.

(iv) There is some evidence that at high doses the macroscopic growth considerably exceeds the theoretical growth but this conclusion was based on theoretical growth figures obtained by Shields et al. (1962) which are not self–consistent (See Section 2.3).

2.3 Lattice Parameter Changes

The first report of the effect of neutron irradiation on beryllium oxide was published by Bacon and Wilson (1955) who showed that in material irradiated to a thermal neutron dose of 7×10^{20} nvt (fast flux and temperature unspecified) the c parameter increased by 0.08 per cent. and the a parameter by 0.03 per

cent. Many workers have since reported lattice parameter changes (Clarke, Tappin, and Ghosh 1961; Elston and Labbe 1961; Elston 1962; Collins, reported by Clarke 1962; Shields et al. 1962). All these workers found that the expansion increased with dose and that the expansion of the $\underset{\sim}{c}$ parameter was greater than that of the $\underset{\sim}{a}$ parameter, but considerable disagreement existed as to the relative magnitude of the changes in the two parameters. For instance, Clarke et al. (1961), reported that $\frac{\Delta \underset{\sim}{c}}{\underset{\sim}{c}}$ was 3 to 4 times $\frac{\Delta \underset{\sim}{a}}{\underset{\sim}{a}}$ whereas Elston and Labbe (1961) found that $\frac{\Delta \underset{\sim}{c}}{\underset{\sim}{c}}$ was 10 to 15 times $\frac{\Delta \underset{\sim}{a}}{\underset{\sim}{a}}$. Elston (1962) noted that the lattice parameter change at 400 °C was less by a factor of about 2 than for the same dose at 100 °C.

There is a disagreement between the United Kingdom and French workers on the effect of annealing. Clarke et al. (1961) reported annealing studies on material irradiated to 3×10^{19} nvt (> 1 MeV) at < 100 °C and found that both the $\Delta \underset{\sim}{c}$ and $\Delta \underset{\sim}{a}$ changes annealed steadily from 200 °C to 1100 °C, whereas Elston (1962) reported little change in $\frac{\Delta \underset{\sim}{c}}{\underset{\sim}{c}}$ in material irradiated at 400 °C to 2×10^{20} nvt (> 1 MeV), until temperatures of 900 – 1000 °C were reached, and even at 1100 °C recovery was far from complete.

Shields et al. (1962) reported $\frac{\Delta \underset{\sim}{c}}{\underset{\sim}{c}}$ changes of up to 7×10^{-3} and $\frac{\Delta \underset{\sim}{a}}{\underset{\sim}{a}}$ changes of up to 1×10^{-3} after irradiation to doses in the range 0.4 to 2.2×10^{21} nvt (> 1MeV) at 100 °C, but the results show little correlation with dose. At similar doses at high temperatures (400 – 1000 °C) the changes were generally smaller than at low temperatures but, again, the results cannot be correlated very well with dose or temperature.

2.4 X–Ray Line Broadening Studies

Shields et al. (1962) reported studies by Yakel of the broadening of X–ray diffraction lines. For specimens irradiated at 120 °C he observed the following:

(i) No broadening of the (h,k,o) reflections.

(ii) Symmetric broadening of the (h,k,l) reflections when $l = 2n$.

(iii) Asymmetric broadening of the (h,k,l) reflections when $l = 2n + 1$.

At high irradiation temperatures the symmetric broadening was still present but there was little asymmetric broadening, although the results were not very consistent.

Clarke (1962) reported that Yakel interpreted these results in terms of defect clusters in the basal planes containing about 15 defects, for low irradiation temperatures, but for irradiation temperatures above 500 °C these clusters were thought to be absent.

Elston and Labbe (1961) also reported broadening of the (h,k,l) reflections for $l \neq o$ and found that in material irradiated at 100 °C the broadening of the (002) reflection started to anneal at 500 °C but annealing was not complete at 1100 °C.

2.5 Mechanical Properties

Elston and Caillat (1958), Elston and Labbe (1961), and Elston (1962) reported results of the effect of irradiation on the compressive strength of hot–pressed beryllium oxide of various densities. Their results may be summarised as follows:

(i) After irradiation at < 100 °C there was a steady reduction in the room temperature compressive strength; for doses above 10^{20}nvt (> 1MeV) the strength was less than one tenth of that of unirradiated material.

(ii) There was some slight evidence that the reduction in strength was less for lower density material.

(iii) Annealing studies showed little recovery until temperatures of 1000 °C were reached and even after long periods at high temperatures the strength did not return to that of the unirradiated material.

(iv) The effect of irradiation at 350 – 400 °C was less than for equivalent doses at 100 °C.

(v) Material irradiated at 400 °C to 2 x 10^{20} nvt (>1 MeV) showed little change in strength when tested at 1000 °C, whereas its room temperature was considerably reduced. In tests at 400 °C there was a reduction in strength but recovery of strength at this temperature was considerable after 24 hours annealing at 400 °C. This contradicts their earlier results and is difficult to understand because the irradiation extended over a period of months at this temperature; a few hours annealing should not produce any changes.

Tobin (1962) reported the results of compressive strength measurements on pure beryllium oxide, and beryllium oxide containing various additives, after irradiation to 1.7 to 2.1 x 10^{21} nvt (>1MeV) at 800 – 980 °C. All materials showed a reduction in strength to about one quarter to one third of the pre-irradiation value. The beryllium oxide containing 1.0 and 2.0 per cent. bentonite showed a smaller change and had higher strengths both in the irradiated and unirradiated condition than the pure beryllium oxide or the beryllium oxide plus magnesium oxide. However there was a very wide scatter in the results and this makes the conclusions doubtful. Material irradiated to similar doses at <800 °C had cracked under irradiation and strength measurements could not be made.

Elston (1962) reported a few results of tensile strength measurements on hot-pressed material after irradiation to 2.2 x 10^{20} nvt (>1 MeV) at 350 – 400 °C. The results showed a reduction in strength by up to a factor of 15. The method of testing was not stated and the anomalous variation of the strength of the unirradiated materials with density makes it difficult to draw any firm conclusions from the results.

Collins, reported by Clarke (1962), measured the crushing strength of hollow hexagonal tubes and found little change up to doses of 1 x 10^{20}nvt (>1 MeV) at a temperature of 100 °C with a steady reduction in strength at higher doses. At 3 x 10^{20} nvt the strength was 50 – 70 per cent. of the unirradiated value.

Clarke et al. (1961) reported a slight increase in modulus of rupture after a dose of 1.5 x 10^{19} nvt (>1 MeV) but did not report any results for higher doses.

Clarke et al. (1961) reported very small changes (less than 1 per cent.) in the resonant frequency and hence presumably in Young's Modulus after doses of 1.5 x 10^{19} nvt (>1 MeV). Elston and Caillat (1958) reported a decrease of 50 – 60 per cent. in Young's Modulus after a dose of about 10^{20} nvt (>1 MeV) at 100 °C. However they used a resonant frequency method for the measurement and reported that the resonant frequencies were barely observable in the irradiated material so the result should be treated with some caution.

2.6 Thermal Conductivity

Elston and Caillat (1958) reported a significant reduction in thermal conductivity at about 0–100 °C after doses of 2.5 x 10^{19} nvt (>1 MeV) at 100 °C and a reduction of 70 – 80 per cent. at 6 x 10^{19} nvt (>1 MeV). At the higher dose the thermal conductivity was almost independent of temperature in the range measured (100 – 220 °C). Annealing at 500 – 600 °C produced some recovery and recovery was complete after annealing at 1400 °C. McGill and Smith (1959) reported no change in the thermal conductivity up to 1000 °C after irradiation to 5 x 10^{20} nvt (thermal) at 185 °C (fast neutron dose was unspecified but probably about 5 x 10^{19} nvt).

Tobin (1962) studied the thermal diffusivity which is related to the thermal conductivity k by $D = \frac{k}{\rho c}$ where ρ is the density and c the specific heat and he assumed that any changes in the thermal diffusity are due to changes in conductivity. He made measurements at 550 °C on pure beryllium oxide and beryllium oxide containing various additives, after irradiation at 1.7 to 2.5 x 10^{21} nvt (>1 MeV) at 800 – 980 °C. The results showed a wide scatter; for instance, nominally identical pellets of beryllium oxide – 1% magnesium oxide gave values ranging from 0.19 to 0.095 cal cm^{-1} sec^{-1} $(deg.C)^{-1}$ before irradiation. Tobin stated that the conductivities after irradiation were 15 – 40 per cent. lower than before irradiation but the wide scatter of results precludes the drawing of any conclusions on the effect of composition, etc.

2.7 Stored Energy

Clarke and Williams (1961) reported no stored energy release up to 500 °C in material irradiated

to 6 x 10^{18} nvt (>1 MeV) at about 100 °C; the limit of accuracy was 0.2 cal/g. Elston (1962), by plunging specimens into a bath at 1132 °C and measuring the temperature drop, measured a release of 14 – 27 cal/g at 1132 °C in material of density 2.86 after irradiation to 2.2 x 10^{20}nvt (>1 MeV) at 400 °C, but there was no significant release in material of density 2.97. He suggested that this difference in behaviour was due to the fact that the lower density specimen had not cracked under irradiation and that the measured energy release was the strain energy associated with the anisotropic growth process. The high density specimen had cracked under irradiation and hence released the strain energy before being tested. However this explanation is difficult to accept as the elastic strain energy is given by $\frac{1}{2}YS^2$ where Y is Young's Modulus and S is the strain and by substituting values for this dose one obtains less than 0.5 cal/g for the strain energy. The quoted figures are the results of only two measurements and it is probable that the apparent discrepancy is due to the measuring technique rather than to a real difference between the specimens.

2.8 Microstructure

Shields et al. (1962) suggested that some irradiation-induced grain growth may occur at doses above 10^{20}nvt even at temperatures as low as 120 °C, but the suggestion is not supported by very conclusive evidence.

Elston (1962) reported that the rate of etching in hydrofluoric acid around the grain boundaries of irradiated material was much faster than that around unirradiated material. The attack appeared to occur preferentially on some grain boundaries.

Frisby, Bisson, and Caillat (1959) examined replicas from fractured surfaces of irradiated beryllium oxide which had been heated to elevated temperatures. They reported void formation at the grain boundaries for temperatures above 1000 °C. At the time they attributed this to the formation of helium bubbles but they have since shown that a similar structure can be produced by heating unirradiated material (Bisson and Frisby 1961).

Shields et al. (1962) showed that voids appear in material irradiated or heat treated at above 1000 °C that are not present in unirradiated material.

During electron microscopic examination of thin sections, Bowen, Wilks, and Clarke (1962) observed dislocation loops in the prism planes after heating material irradiated at 100 °C to above 1000 °C.

2.9 Behaviour of Helium and Tritium

Aslanian et al. (1961) investigated the diffusion of helium in irradiated beryllium oxide by measuring the specific heat at liquid helium temperatures after annealing material irradiated to 2.2 x 10^{20} nvt (>1 MeV). He first noticed a specific heat anomaly corresponding to the lambda transformation in helium after annealing at 600 °C, and a very marked anomaly was observed after annealing at 1200 °C. This suggests that helium diffuses to voids at temperatures as low as 600 °C although Aslanian did not make any quantitative measurements to determine whether a significant fraction of the helium was producing the observed effects.

Shields et al. (1962) measured the helium and tritium concentrations in beryllium oxide irradiated up to doses of 2 x 10^{21} nvt (>1 MeV) at 100 – 1000 °C. They concluded that little, if any, helium escaped from the specimens for any condition, but, for irradiation temperatures above 500 °C, most of the tritium escaped from all specimens. This is not surprising in view of the likely high diffusion coefficients of tritium.

3. EXPERIMENTAL METHODS

3.1 Material

The specimens were fabricated by the Ceramics Group at Lucas Heights and full details of the methods used have been given by Reeve and Ramm (1961a and 1961b), and Ramm and Reeve (unpublished). Briefly the following methods were used:

Hot Pressing: Pechiney nuclear grade beryllium oxide was hot pressed in graphite dies at pressures of 1 ton/in^2 and temperatures of 1750 °C for periods of half an hour. This resulted in material of 96 – 98 per cent. theoretical density with a mean grain size of 10 – 30μ. Translucent material of almost theoretical

density was fabricated by pressing Berylco No. 1 beryllium oxide at 1600 – 1700 °C at 1 ton/in^2 for four hours. This material had a mean grain size of 25 – 30μ.

Cold Pressing and Sintering: Brush UOX beryllium oxide was hydrostatically pressed without a binder at 20 tons/in^2 and sintered in dry flowing air for one hour at various temperatures between 1200 and 1550 °C to provide specimens with different densities and grain sizes. To obtain fine-grained specimens, the "as-received" powder was ground before being compacted. Details of techniques together with densities and grain sizes are:

(i) As-received material sintered for 1 hour at 1500 °C, 95 – 96 per cent. theoretical density. Mean grain size 20 – 30μ.

(ii) As-received material sintered for 1 hour at 1200 °C, 72 – 75 per cent. theoretical density. Mean grain size $<1\mu$.

(iii) Pre-ground material sintered for 1 hour at 1400 – 1500 °C, 90 – 94 per cent. theoretical density. Mean grain size $<2\mu$.

(iv) Pre-ground material sintered for 1 hour at 1500 – 1550 °C, 95 – 97 per cent. theoretical density. Mean grain size $<3\mu$.

(v) Pre-ground material sintered for 1 hour at 1550 °C, 97 – 98 per cent. theoretical density. Mean grain size 7.5 – 15μ.

Details of the various types of specimens are summarised in Table 2 and a letter code is allocated to each group. These letters are for reference to each group throughout this report.

Specimens were ground to finished size and in the case of the pre-ground cold-pressed and sintered specimens (Groups D, E, and C) each specimen was individually examined to determine the mean grain size.

Specimens of three main types were used:

(i) Cylinders 0.3 inch dia. x 0.6 inch long for dimension, X-ray, thermal conductivity, and compressive strength measurements, and metallography.

(ii) Rectangular specimens 0.15 inch x 0.25 inch x 1 inch for bend tests and X-ray measurements.

(iii) Cylinders 0.75 inch dia. x 0.75 inch long for neutron scattering measurements.

3.2 Irradiation Techniques

The specimens examined to date have been irradiated at either pile temperatures (60 – 100 °C) or at temperatures in the range 500 – 700 °C. The two types of rigs used for these irradiations are described in the following sections. Full details of the specimens irradiated in each rig and the dose and irradiation temperature to which they were subjected are given in Table 3.

3.2.1 Pile temperature irradiations

In early irradiations at pile temperatures the specimens were held in carriers, packed in aluminium powder, and contained in an aluminium tube which was immersed directly into the heavy water. Thermo-couples were strapped to the specimens at intervals along the length of the rig and these indicated that the specimen temperatures were generally in the range 60 – 80 °C with some in one rig (X-4) reaching 125 °C. These irradiations were carried out in either the 2V-3 heavy water position or the C-3 hollow fuel element position in HIFAR. In later irradiations the specimens were packed with aluminium powder and sealed in aluminium cans. These cans were loaded into, and unloaded from, a permanent irradiation facility (X-75), in the C-3 hollow fuel element position, by retracting the facility into a handling flask situated on the storage block. Temperature measurements were not made in this facility, sufficient experience having been gained with the earlier type of rig to guarantee that the irradiation temperatures would be in the range 60 – 100 °C. Throughout this report the pile temperature irradiations are referred to as "irradiation at <100 °C".

3.2.2 High temperature irradiation

The type of rig for irradiation at elevated temperatures is shown schematically in Figure 1. Specimens were supported in carriers in a stainless steel can which was filled with pure helium under reduced pressure. A Nichrome resistance furnace was wound on the outside of this can either on Refrasil insulation (Rig X–5) or pyrophyllite ceramic formers (Rig X–73). The furnace unit was contained in a splined aluminium former which allowed the passage of heater leads and thermocouples. Mineral–insulated thermocouples placed centrally in the top and bottom of each can were used to measure and control temperature. In Rig X–73 a third thermocouple placed eccentrically, was included in each can to measure the radial temperature gradient in the can.

In each rig there were three furnace units contained in an outer aluminium tube which was immersed directly into the heavy water. The temperature of each furnace was controlled using a proportional potentiometer recorder controller operating a magnetic amplifier and saturable reactor to control the heat input to each furnace unit. Control of temperature at the thermocouple position was generally maintained to $\pm 5\,^{\circ}C$ during pile operation but owing to uneven gamma–heating effects, considerable longitudinal temperature gradients of up to $30\,^{\circ}C$ existed in each can. Axial temperature gradients were generally found to be less than $10\,^{\circ}C$.

In the first rig of this type (X–5) the centre furnace unit failed during out–of–pile testing but the irradiation was proceeded with, the gamma–heating alone being sufficient to give this unit a useful operating temperature.

In the second rig of this type (X–73) the centre furnace unit failed after one reactor operating period and the lower furnace unit after two periods. However gamma–heating was again sufficient to raise the temperatures to useful values during pile operation. Operating temperature ranges for each group of specimens referred to in this report were estimated from the temperature charts.

3.2.3 Flux Monitoring

Integrated neutron fluxes were estimated from data on the thermal to fast flux ratios obtained during low power operation of HIFAR and from cobalt thermal flux monitors incorporated in each rig. The activity of the cobalt monitors was measured after irradiation by comparison with a standard monitor using a constant–geometry gamma–spectrometer. The standard monitor had been calibrated against a monitor whose absolute activity was determined by dissolution followed by $4\pi\beta$ counting and by using a calibrated electrometer. For the short term irradiations the fast flux figures obtained by this method were checked, with good agreement, by nickel monitors; the Co–58 activity arising from the $^{58}Ni\ (n,p)^{58}Co$ reaction was estimated using beta–gamma coincidence counting methods. All the fluxes quoted in this report, unless otherwise specified, are the integrated fluxes over the fission neutron spectrum. The relative values for the hollow fuel element irradiations are probably accurate to $\pm 10 - 15$ per cent. but the absolute fluxes and the values for the 2V–3 irradiations may have a larger error than this owing to uncertainties in the shape of the neutron energy spectrum. The fluxes above 1 MeV would be approximately 70 per cent. of the quoted values. The flux spectrum for the hollow fuel element positions, where the majority of the irradiations were carried out, is shown in Figure 2. This spectrum was obtained by Lang (1962) by combining data from resonance and threshold detectors with calculated data.

3.3 Metrology and Density Measurements

Dimension measurements were made to an accuracy of ± 0.0001 inch using a vernier micrometer. Density measurements were made by the displacement method in n–octyl alcohol after first outgassing and impregnating the specimen in the alcohol under vacuum. Porosity was estimated from these data by using the relationships:

$$P_T = 1 - \frac{D_B}{D_T} \quad ,$$

$$P_o = 1 - \frac{D_B}{D_A} \quad ,$$

$$P_c = P_T - P_o \quad ,$$

where P_T = total porosity

P_o = open porosity

P_C = closed porosity

D_B = bulk density obtained by weighing and measuring the dimensions of the specimen

D_T = theoretical density obtained from X-ray lattice parameter measurements

D_A = apparent density measured by displacement as described above.

3.4 Mechanical Testing

Bend tests were made at room temperature with 2 cm between the outer knife edges at a strain rate of 0.0001 inch/minute using a 3 point load fixture. Compression tests were made at room temperature at a strain rate of 0.0001 inch/minute in an Instron machine.

3.5 Thermal Conductivity

Thermal conductivity measurements were made by a comparative method in which the temperature drop along part of the specimen was compared with the temperature drop in a piece of pure iron. The method has been described in detail by M.K. Cooper, A.R.Palmer, and G.Z.A. Stolarski (A.A.E.C. unpublished).

3.6 X-Ray Measurements

Techniques used for studying X-ray parameter changes and line broadening have been described in detail by Hickman et al. (1962). Briefly, parameter changes were measured on solid specimens by comparing the positions of the peaks of selected reflections from the irradiated and unirradiated material using a diffractometer. For the a parameter change the (300) Cu $K\alpha_1$ reflection was used and for the c parameter change the (213) Cu $K\beta$ was generally used, other reflections being measured on some specimens. Line broadening due to irradiation was measured by subtracting the integral line breadth of the unirradiated material, as obtained from the diffractometer trace, from that of the irradiated material. Absolute lattice parameters were determined in some cases by an extrapolation technique and the values for the lattice parameter changes obtained by this method were in good agreement with those obtained by the line shift method (D.G.Walker A.A.E.C. unpublished).

3.7 Long Wavelength Neutron Scattering

Long wavelength neutron scattering experiments were carried out using a neutron spectrometer described by Sabine et al. (1962). The transmission of neutrons of wavelength 4.5 – 9.0 Å through the irradiated specimens was compared with that through an identical set of unirradiated specimens.

3.8 Out-of-Pile Controls

Control specimens for the elevated temperature irradiations were subjected to the same thermal history as that received by the in-pile specimens. They were canned in stainless steel in an inert helium atmosphere for this heat treatment.

4. RESULTS

4.1 Macroexamination

All specimens were generally discoloured by irradiation; the white cold-pressed and sintered specimens turned grey-black and the grey hot-pressed material turned a darker shade of grey. The translucent material turned grey and became opaque.

Macroexamination at magnifications up to X15 failed to show any cracking or distortion except in two materials irradiated at $<100\,^{\circ}C$. Details of these two cases are as follows:

(i) Hot-pressed Pechiney beryllium oxide (material A) irradiated to doses of $3.5 - 6.5 \times 10^{20}$ at $<100\,^{\circ}C$ (Rig X-39). These specimens showed various degrees of cracking and powdering from complete disintegration to powder to a slight crumbling at the corners (Figure 3). These latter samples were very friable and, when they were handled with manipulators powdered material was rubbed off the surface. Many specimens were found to be cracked on decanning. This cracking was often axial and it was always associated with at least some degree of

powdering. Some specimens which were not cracked on decanning subsequently cracked during handling.

(ii) Translucent beryllium oxide (material B) irradiated to 5 x 10^{20} at $<100\,^{\circ}C$ (Rig X-75). These specimens were found to have partly crumbled during irradiation (Figure 4) and further crumbling occurred during post-irradiation handling. Microscopic examination of the powder from crumbled specimens showed that the particle size was of the same order as the original grain size.

Hot-pressed Pechiney material A irradiated with the translucent specimens showed no macroscopic evidence of cracking but X-ray and metallographic examination indicated the presence of extensive micro-cracking in this material. (See Sections 4.4 and 4.8).

4.2 Dimension Changes

The results of dimension measurements before and after irradiation are summarised in Table 4 and the results for some materials are plotted in Figures 5 and 6. The volume changes quoted in this table are calculated from the dimensions $\left(\frac{\Delta V}{V} \approx \frac{2\Delta d}{d} + \frac{\Delta l}{l}\right)$. It was difficult to make measurements on the cracked and crumbled specimens but those which were possible and which were considered significant have been included in Table 4. The results showed the following features:

(i) In hot-pressed material irradiated at pile temperatures, the growth increased in a fairly linear manner with dose up to about 10^{20} nvt; above this dose the expansion became relatively greater than at lower doses. (See Figure 5).

(ii) The percentage increase in diameter of the hot-pressed materials A and B was greater than the percentage increase in length. The coarse-grained cold-pressed and sintered material C also showed this effect to some extent but the expansion of the fine-grained cold-pressed and sintered materials was uniform.

(iii) The expansion of the cold-pressed and sintered material was much less than hot-pressed material at the same dose both for elevated and pile temperature irradiations. The expansion of the fine-grained cold-pressed and sintered material was somewhat less than that of the coarse-grained material at the same dose. The lower density, fine-grained material expanded somewhat more than the corresponding higher density material although these differences were only just significant.

(iv) The expansion after irradiation at 500 - 700 °C was much smaller by a factor of three to five than for the same dose at $<100\,^{\circ}C$. (See Figure 6). There was some indication that in materials A and F the expansion decreased with temperature in the range 500 - 700 °C; however this was not observed in material G, the low density cold-pressed and sintered material, which showed the reverse effect.

The recovery of the dimension changes on annealing was studied using material A irradiated to 1.8 x 10^{20} nvt at $<100\,^{\circ}C$ and the results are shown in Figure 7. There was a slight recovery up to 1000 °C (about 30 per cent) but at 1400 °C recovery was only 60 per cent. complete. However, control specimens heat treated with the irradiated specimens showed a volume expansion in the region 1200 - 1400 °C of up to 0.15 per cent. This was shown to be due to void formation resulting from reaction of air with included carbon (K.D.Reeve and J. Chute A.A.E.C. unpublished) and this explains the apparent non-recovery of the irradiation induced growth.

No dimension changes of any significance could be detected in any of the control specimens subjected to the same thermal history as the irradiated specimens in the reactor.

4.3 Porosity Changes

Owing to porosity and changes in porosity of most specimens, density measurements using a liquid displacement technique have not much significance but they do allow estimates of open and closed porosity and the changes in these quantities on irradiation. The results are shown in Table 5. The measured porosities were accurate to approximately ± 0.3 per cent. The main interesting feature of these results is the large increase in open porosity which occurred in hot-pressed material, particularly after irradiation to high doses at pile temperatures. The fine-grained cold-pressed and sintered

materials D and E showed no significant increase after 3 x 10^{20} nvt at pile temperatures and material D actually showed a decrease at 5 x 10^{20} nvt. The coarse-grained cold-pressed and sintered material C showed no change at 3 x 10^{20} nvt but an increase in open porosity at 5 x 10^{20} nvt. At higher temperatures both high density materials (A and F) showed increases in open porosity, the increase generally being larger in the hot-pressed material. The porosity of the low density material G was virtually all open porosity both before and after irradiation.

4.4 X-Ray Diffraction Studies

Early X-ray diffraction work was reported in detail by Hickman et al. (1962). The lattice parameter changes obtained since then, together with the earlier results, are summarised in Table 6, and the theoretical growth calculated from these data is compared with the macroscopic growth in Table 4. The results for irradiation at 100 °C are plotted in Figures 8 and 9. The quoted results are generally the mean of two specimens for each condition; if these differed by more than the experimental error then the results were quoted separately. The main features observed were as follows:

(i) At pile temperatures $\frac{\Delta \underset{\sim}{c}}{\underset{\sim}{c}}$ was always considerably larger than $\frac{\Delta \underset{\sim}{a}}{\underset{\sim}{a}}$ but the absolute and relative values of the changes varied considerably from one material to another and from one condition to another. This is apparent from Figures 8 and 9. First, at low doses both parameters in material A increased in an approximately linear manner with dose on the log-log graph until a dose was reached where the $\frac{\Delta \underset{\sim}{c}}{\underset{\sim}{c}}$ was larger and $\frac{\Delta \underset{\sim}{a}}{\underset{\sim}{a}}$ was smaller than would be expected from the results at lower doses. This behaviour is interpreted in terms of changes in the parameters resulting from powdering (see later), which is confirmed by the increase in $\frac{\Delta \underset{\sim}{c}}{\underset{\sim}{c}}$ and the decrease in $\frac{\Delta \underset{\sim}{a}}{\underset{\sim}{a}}$ which resulted from crushing material irradiated to 9 x 10^{19} nvt. Secondly, a marked effect of grain size on the actual values of the lattice parameters can be seen by examining the results for the various materials irradiated to 3 x 10^{20} nvt. Fine-grained materials E and F showed much smaller changes in $\frac{\Delta \underset{\sim}{c}}{\underset{\sim}{c}}$ than the coarse-grained materials. It might be claimed that the results indicate a tendency towards saturation of the $\underset{\sim}{a}$ parameter change but it is considered that this apparent effect arises from the complicating effect of crumbling on the $\underset{\sim}{a}$ parameter. Examination of the results for material E irradiated to 3 and 5 x 10^{20} nvt, and comparison of the results for crushed material A at 9 x 10^{19} nvt with those of the crumbled material A at 3 x 10^{20} nvt do not support this hypothesis; the results show that in the absence of complications due to crumbling the $\underset{\sim}{a}$ parameter was still increasing with dose at about the same rate as at lower doses.

(ii) The changes in the $\underset{\sim}{c}$ parameter after irradiation at about 500 °C were approximately a factor of three smaller than for equivalent doses at 100 °C and at 650 – 700 °C they were smaller by a factor of about five. The changes in the $\underset{\sim}{a}$ parameter after irradiation at 500 – 700 °C were generally very small. It was noted that for these high temperature irradiations there was a significant $\underset{\sim}{a}$ parameter change only where there was broadening of the (300) reflection; in the cases where the $\underset{\sim}{a}$ parameter change was insignificant, no significant (300) line broadening could be observed. (Compare for instance the results for the two sets of specimens of material A irradiated to 5 x 10^{20} nvt at 500 – 600 °C (Table 4)). The $\underset{\sim}{a}$ parameter changes observed after irradiation to 1 – 1.5 x 10^{20} at 500 – 700 °C were generally equal to, or greater than, the changes observed at higher doses (5 – 7 x 10^{20}) at the same temperatures, suggesting that there was a saturation effect. There was no evidence for saturation of the $\underset{\sim}{c}$ parameter changes although this could occur at higher doses.

(iii) The results of isochronal annealing studies on material A irradiated to 9 x 10^{19} nvt and 3.5 x 10^{20} at <100 °C are shown in Figure 11. The $\underset{\sim}{a}$ parameter recovery commenced at 200 °C and was virtually complete by 1000 °C, the higher dose material recovering somewhat faster than the lower dose material. Little recovery of the $\underset{\sim}{c}$ parameter occurred until temperatures of 800 °C were reached and recovery was not complete until 1400 °C. Isothermal annealing studies have only been done at 600 °C. These showed that all the recovery which occurred at this temperature took place in the first hour and no further recovery could be detected in periods of up to 100 hours.

(iv) Line broadening of all (h,k,l) lines for $l \neq 0$ occurs and increases with dose. At high doses this broadening is very extensive and makes measurement of the $\underset{\sim}{c}$ parameter change difficult and in some cases impossible. (See Figure 10). This broadening was observed in material irradiated at both pile temperature and at 500 – 700 °C. In material irradiated at pile temperatures the broadening anneals in the range 1000 – 1400 °C (Figure 11).

(v) Line broadening of all (h,k,o) lines occurred and increased with dose up to the dose where crumbling and powdering occurred; at that dose no broadening was observed although there was a loss in intensity. The broadening of the (300) line, which is typical of this effect, is included in Table 6 with the lattice parameter results. It will be noticed that:

(a) There was no (300) broadening for hot–pressed material irradiated to 3×10^{20} nvt and above at pile temperatures, and for some specimens irradiated to 5×10^{20} nvt and above at elevated temperatures.

(b) The coarse–grained cold–pressed and sintered material C showed less (300) broadening at 5×10^{20} nvt than at 3×10^{20} nvt.

(c) The fine–grained cold–pressed and sintered materials D and E showed (300) broadening which increased with dose and, at 5×10^{20} nvt, was very extensive and resulted in almost complete elimination of the high angle lines.

(d) At 3×10^{20} nvt the coarse–grained material C showed more broadening than the fine–grained material D and E.

(e) The (300) broadening in material A irradiated to 9×10^{19} nvt at pile temperatures annealed out in the range 800 – 1200 °C, that is, in much the same temperature range as the $\underset{\sim}{c}$ parameter annealed but in quite a different range to the $\underset{\sim}{a}$ parameter.

(f) For irradiation at 500 – 700 °C, (h,k,o) broadening was present in all cases except in some hot–pressed specimens irradiated to $5 - 7 \times 10^{20}$ nvt at 500 – 700 °C. The broadening, when present, was less than for the same dose at pile temperatures.

(vi) Material irradiated to 1.5×10^{20} nvt at 640 – 660 °C showed very anomalous behaviour with wide variations in both parameter changes and line broadening for nominally identical specimens.

4.5 Mechanical Properties

Only a very limited amount of work has been done to date on mechanical property changes after irradiation, but a more extensive programme is now under way. Some measurements of the room temperature modulus of rupture using a three–point bend test have been made on hot–pressed material A and the results are shown in Table 7. Significant changes occurred only in material irradiated to 3.5×10^{20} nvt at pile temperatures in which crumbling had started, and which had virtually no strength, and in three of the four specimens irradiated to 1.5×10^{20} nvt at 640 – 660 °C where there was a considerable reduction in strength. However, owing to the small number of specimens tested at each condition, and the wide scatter of results for the 640 – 660 °C irradiation, not too much reliance should be placed on these data although they do suggest that there is little change in strength up to doses of about 1×10^{20} nvt at pile temperatures. As was noted earlier the hot–pressed material irradiated to 1.5×10^{20} nvt at 640 – 660 °C also showed anomalous lattice parameter and X–ray line broadening effects.

A limited number of compression tests were made on specimens of hot–pressed material A after all other measurements had been completed; the results are shown in Table 8. Again little reliance can be placed on these results owing to the low number of specimens tested at each condition, the very wide scatter of results even in unirradiated material, and the low length to diameter ratio of the specimens, which was not ideal for compression testing.

4.6 Long Wavelength Neutron Scattering

The results of the long wavelength neutron scattering studies are presented in detail by Sabine, Pryor, and Hickman (1962). The measurements depend on the fact that for neutron wavelengths beyond the Bragg cut–off, where coherent elastic scattering is eliminated, the defect scattering cross section forms a major part of the total scattering cross section and is equal to the bound atom cross section. By comparing the transmission of long wavelength neutrons through identical irradiated and unirradiated specimens, the extra defect scattering induced by irradiation can be measured directly. Analysis of this extra scattering and its wavelength dependence provides information about the number of defects and their distribution. Measurements were made on hot–pressed material A after irradiation to doses of 1×10^{19} nvt to 6.8×10^{20} nvt at < 100 °C, and after irradiation to about 1×10^{20} nvt at 500 – 700 °C. The effect of annealing on specimens irradiated to 1.8×10^{20} nvt at < 100 °C was also studied. The

results showed a considerable amount of defect scattering which increased with dose and showed a very strong wavelength dependence. Analysis of the results led to the following conclusions:

(i) Dilatation around isolated defects cannot alone account for the observed wavelength dependence of the scattering suggested by Martin (1960).

(ii) A model in which approximately half the defects are present in clusters containing a minimum of 15 interstitials or vacancies and the other half randomly distributed describes very closely the observed wavelength dependence of the scattering.

(iii) Calculations of defect concentration using the above model give the values shown in Table 9. Also shown in the table are the calculated number of primary knock–ons resulting from collisions of fission neutrons (assuming an averaged cross section for beryllium and oxygen over the fission spectrum) and the number of displacements per primary knock–on. It can be seen that the defect concentration increased in a fairly linear manner with dose up to the highest dose investigated and that the number of displacements per primary collision was of the same order at all doses although there is some indication that the number may have been higher at the lower doses.

(iv) It is quite possible that the assumed model is oversimplified but any reasonable variations in the model will not affect the defect concentration figures by more than ± 50 per cent.

(v) Little annealing of defects appears to have occurred until temperatures of 800 °C were reached. Annealing was complete by 1400 °C. (See Figure 11).

(vi) The results obtained on specimens irradiated to about 1 x 10^{20} nvt at 500 – 700 °C were not very accurate owing to the small size of the specimens but they indicated that extra scattering also occurred and that this scattering showed the same strong wavelength dependence as for the material irradiated at <100 °C.

More recently, measurements have been made on coarse–grained material C fabricated by cold–pressing and sintering and irradiated to 3 x 10^{20} nvt at <100 °C (T.M.Sabine A.A.E.C. unpublished). The results were in close agreement with those obtained previously for hot–pressed material.

4.7 Thermal Conductivity

Early work on the effect of irradiation on the thermal conductivity of hot–pressed material A in the range 10 – 100 °C has been reported in detail by M.K. Cooper, A.R. Palmer, and G.Z.A. Stolarski (A.A.E.C. unpublished). More recently measurements were made on material A and cold–pressed and sintered materials F and G irradiated to higher doses at elevated temperatures (P.M.Heuer, G.Z.A.Stolarski, and A.W.Pryor, A.A.E.C. unpublished). The results of these measurements for the conductivity at 45 °C are summarised in Table 10. The main features of these experiments were as follows:

(i) In irradiation at both pile and elevated temperatures, the conductivity decreased steadily with increasing dose but the increase after irradiation at 500 – 700 °C was less by a factor of about three than for equivalent doses at pile temperatures.

(ii) For doses above 2 x 10^{19} nvt at pile temperatures the thermal conductivity was virtually independent of temperature over the measured range, in contrast to the marked temperature dependence in unirradiated material. This temperature independence was also evident in all the specimens irradiated at elevated temperatures except those irradiated at 610 – 630 °C to 1.1 x 10^{20} nvt and at 650 – 670 °C to 1.5 x 10^{20} nvt (that is, to the lower doses at high temperatures).

(iii) Annealing studies of material A irradiated at pile temperatures showed no recovery until 600 °C and then a fairly steady recovery until all the damage was annealed at 1400 °C. (See Figure 11).

(iv) The limited amount of available data about cold–pressed and sintered material suggests that, although it has a somewhat lower conductivity to start with, the reduction on irradiation is less than for hot–pressed material. The variation of conductivity with density in this material is somewhat anomalous and cannot be explained simply in terms of the fraction of pores. P.M.Heuer et al. suggest that this may be due to the nature of the pore structure and that the apparently smaller changes on irradiation may be due to changes in this pore structure.

(v) The extra thermal resistance introduced by irradiation (defined by $W = \frac{1}{K_I} - \frac{1}{K_u}$ where K_I and K_u are the conductivities of the irradiated and unirradiated material respectively) has been calculated by P.M.Heuer et al. from the above measurements and also from measurements on the same specimens by Dr. G.K. White of C.S.I.R.O. at temperatures down to 4 °K. These showed that, in the absence of annealing, the thermal resistance introduced by irradiation was inversely proportional to temperature and it is therefore suggested that the reduction in thermal conductivity at temperatures of interest in a reactor system (500 – 1000 °C) will be much less than the reduction in room temperature conductivity. Results of their estimates of conductivities at higher temperatures based on these arguments are shown in Table 11.

4.8 Metallography

Only a limited amount of metallography work has been done (P. Davis A.A.E.C. unpublished). Further work is in progress. The following features have been observed:

(i) A limited amount of microcracking was observed in most materials in the unirradiated condition. This was not immediately obvious in examination of polished surfaces but examination of the interior with polarised light showed the presence of some microcracks. This microcracking was more extensive in the hot–pressed material than in cold–pressed and sintered material where it was very seldom observed, and was nearly always intergranular.(Figure 12(a)).

(ii) Hot–pressed materials A and B irradiated to 3 x 10^{20} nvt at <100 °C showed very extensive intergranular and some transgranular cracking with almost complete separation of the grains (Figure 12). Even after prolonged polishing many grains were torn out of the surface.

(iii) Hot–pressed material A irradiated to less than 1.5 x 10^{20} at <100 °C and at 500 – 700 °C showed little more microcracking than was present in the unirradiated material.

(iv) Coarse–grained cold–pressed and sintered material C irradiated to 5 x 10^{20} nvt at <100 °C showed fairly extensive intergranular cracking (Figure 12) but it was less than that in hot–pressed material at 3 x 10^{20} nvt, in agreement with the X–ray observations. Coarse–grained material C showed very little cracking after 3 x 10^{20}nvt at <100 °C.

(v) Hot–pressed, and coarse–grained cold–pressed and sintered material F, irradiated to 7 x 10^{20} nvt at 660 – 690 °C, showed some microcracking.

(vi) No useful information could be obtained from examination of the fine grained materials by optical metallography.

4.9 Electron Microscopy

J. Chute (A.A.E.C. unpublished) has done a limited amount of examination of the edges of chips of irradiated hot–pressed material A by transmission in the electron microscope. In some chips irradiated to 3.5 x 10^{20} nvt at pile temperatures a large number of black dots could be observed, some of which could be resolved into loops. Owing to the unsatisfactory nature of chips for examination by transmission, further work on this problem has been suspended until suitable thin films of beryllium oxide can be prepared.

4.10 Other Measurements

Troup and Thyer (1962) have made electron spin resonance measurements on material A irradiated under various conditions. They detected an anisotropic spin resonance signal whose intensity increased with neutron dose. They found that the signal annealed out in the range 400 – 800 °C. Further work with gamma– and neutron–irradiated single crystals and polycrystalline material has given somewhat confusing results which require further work for their elucidation (G.J.Troup unpublished). In all cases a resonance was obtained which is thought to have been due to positive ion vacancies but several other unidentified resonances were also observed.

5. DISCUSSION

5.1 Growth and Powdering

It appears to be fairly clear that, at least at low doses, the observed macroscopic growth was a direct result of the lattice expansion observed by X–ray methods. In Figure 13 the theoretical growth is

compared with the macroscopic growth for hot-pressed material A. At low doses agreement is good but at doses above 10^{20} nvt the macroscopic growth exceeds the theoretical growth. The only cold-pressed and sintered material examined had received doses exceeding 10^{20} nvt but Table 4 shows that in this material at these doses macroscopic growth exceeded the theoretical growth; however the discrepancy was not as great for hot-pressed material and in many cases was barely significant.

As mentioned in Section 2.2 Clarke (1962), by comparing observations from different laboratories, suggested that this discrepancy existed and that it was due to saturation of the theoretical growth. He postulated that this resulted from the aggregation of defects into new planes which were bounded by dislocation loops. He stated that these would not affect the theoretical growth but would cause macroscopic growth. The present results do not support this hypothesis because:

(i) There is no real evidence for saturation of the theoretical growth. In fact the discrepancy appears to arise mainly from an increasing rate of macroscopic growth rather than a decreasing rate of theoretical growth.

(ii) This phenomenon would be expected to be independent of grain size effects and hence the discrepancy should be the same in fine-grained as in coarse-grained material.

Since the discrepancy was greatest in material which had cracked and crumbled under irradiation and since porosity measurements on this material showed large changes in the amount of open porosity, it is proposed that the discrepancy was due to changes in the pore structure resulting from the anisotropic growth process -- mainly the development of intergranular cracks. This is supported by the metallographic examination in the case of materials irradiated at $<100\,^{\circ}C$. The limited metallographic examination of materials irradiated at $500 - 700\,^{\circ}C$ to $5 - 7 \times 10^{20}$ nvt does not show sufficient difference in the amount of microcracking to explain the large differences in macroscopic growth between hot-pressed and cold-pressed and sintered material but further work on this is proceeding. Although dislocation loops may be present, as indicated by the electron microscope studies, it is not considered to be necessary to invoke them in order to explain the observed results.

The observed lattice expansion must be a direct result of defects produced by fast neutron bombardment rather than the effect of impurity atoms resulting from the (n, 2n) and (n, α) reactions. In Table 12 the defect concentration, obtained from the long wavelength neutron scattering work, is compared with the measured volume expansion obtained by interpolation and extrapolation from the X-ray data. It can be seen that an expansion of approximately 1 atomic volume per defect pair is produced which is of the same order as that found in other materials. The concentration of helium and tritium is two orders of magnitude lower than the defect concentration and could not possibly produce the observed lattice expansion.

Although no direct evidence from single crystals is yet available, it seems that the anisotropic lattice expansion must give rise to a corresponding anisotropic growth of individual grains and that powdering is a direct result of the strains produced by the anisotropic growth of the individual grains in the polycrystalline aggregate. The stress resulting from anisotropic growth in a polycrystalline material will be extremely complex and depend on a number of factors such as grain size, shape, and preferred orientation. However one can consider the simple case of a bicrystal with the $\underset{\sim}{c}$ axis in one grain parallel to the $\underset{\sim}{a}$ axis in the other and assume that a strain is produced equal to the difference in growth in the two crystallographic directions. For specimens of material A, for instance, irradiated to 9×10^{19} nvt at $<100\,^{\circ}C$, this strain would be 0.15 per cent. and, assuming a shear modulus of 20×10^{6} p.s.i., a stress of 30,000 p.s.i. would result. The criterion for failure due to the stresses is somewhat uncertain; it will certainly not be the tensile strength of a bulk specimen (about $25 - 30{,}000$ p.s.i. for this material). However, although the grain boundary cohesive strength is probably considerably higher than 30,000 p.s.i., it is not surprising that microcracking and powdering occurred at higher doses. Either trans-granular or intergranular cracking would relieve the anisotropic growth stresses; however the recovery of the (300) X-ray line broadening, which was observed to be associated with crumbling, would suggest that the cracking was predominantly intergranular, and this is supported by the microscopic observations.

Grain size would appear to be the predominant factor in determining the dose at which crumbling occurs, fine-grained material being able to withstand much higher doses than coarse-grained material. If, as is thought, the broadening of the (300) reflection can be taken as a measure of the internal strain, then it would appear that the internal strains build up at a slower rate in the fine-grained material, are relatively more effective in modifying the lattice parameter changes, and hence in reducing the degree of

anisotropic growth, and the material can withstand a higher degree of internal strain before crumbling. This last effect can be understood by considering the relationship between the critical Griffith crack size and the grain size. In the coarse-grained material the length of the boundary between two highly misoriented grains would generally be of the same order as the critical crack size, so that should a crack be produced on this boundary it could propagate through the material. However in the fine-grained material the length of this boundary would be considerably less than the critical size and a crack, if formed, would not propagate. The earlier onset of powdering in hot-pressed materials A and B compared with the coarse-grained cold-pressed and sintered material C was probably a result of a combination of two effects, namely the slightly coarser grain size of the hot-pressed material and the greater extent of microcracking present in this material before irradiation.

It cannot be claimed that the predominance of the grain size effect in determining the resistance to crumbling has been established beyond all doubt, as the conclusion mainly results from a comparison of coarse grain size material, prepared from Pechiney powder by hot-pressing, with fine grain size material, prepared from Brush powder by cold-pressing and sintering, so the effect could possibly be due to impurities or fabrication method. However since the impurity levels were not much different, the structure of the materials was similar, and some irradiation cracking was observed in the coarser grained cold-pressed and sintered material at 5×10^{20} nvt it is thought that the grain size effect has been established. Comparison of cold-pressed and sintered material of different grain size at higher doses and hot-pressed Brush UOX material of different particle sizes (at present under way) should confirm this conclusion beyond doubt. This strong dependence of powdering on grain size explains why there are wide variations in the observations by overseas workers of the dose at which powdering starts (see Section 2.1).

The macroscopic cracking observed in large diameter (¾ inch) specimens of material A irradiated to $4-6 \times 10^{20}$ was probably the result of thermal stress combined with the weakening of the material due to microcracking. These specimens were subjected to gamma-heating of the order of 2 watts/g. Using the values for the thermal conductivity of irradiated material one obtains a stress of about 2000 p.s.i. so, considering the friable state of the material, it is not surprising that thermal stress cracking occurred.

The suggestion made in an earlier publication (Hickman, Sabine, and Coyle 1962) that the intergranular strain affected the actual values of the measured lattice parameter changes is well supported by the additional results given in this report. It was based mainly on the following facts:

(i) In material which had crumbled under irradiation the $\frac{\Delta c}{c}$ was greater and the $\frac{\Delta a}{a}$ was less than would have been predicted from the results at lower doses on solid material.

(ii) The broadening of the (300) line increased with dose in solid material but was negligible in powdered material.

(iii) An increase in $\frac{\Delta c}{c}$ and decrease in $\frac{\Delta a}{a}$ occurred as a result of crushing material which had not crumbled under irradiation.

These facts suggested that in solid material, as a result of the intergranular strains, $\frac{\Delta c}{c}$ would be less, and $\frac{\Delta a}{a}$ would be greater than for powdered material irradiated to the same dose, and that the (h,k, o) line broadening was a direct result of this intergranular stress. James (1948) suggested that line broadening, β, is related to strain, ϵ , by the relationship:

$$\epsilon = \beta \cot \theta.$$

Substituting the value for β for the (300) reflection obtained from specimens of material A irradiated to 9×10^{19} nvt one obtains a mean strain of 0.1 per cent. which is of the same order as that estimated from the lattice parameter changes. In the fine grained material at higher doses the mean strains are 0.4 to 0.5 per cent. Although these absolute values must be treated with some caution because the James formula is based on an over-simplification of the phenomenon, they do tend to confirm that the (300) line broadening was due to strain and that at the higher doses there was a very high degree of internal strain in the material.

The very marked effect of grain size on the lattice parameter changes is consistent with the above picture. The $\frac{\Delta c}{c} / \frac{\Delta a}{a}$ ratio is found to be smallest in the very fine grained material where,

because of much greater grain boundary area/volume ratio, the intergranular strains are more effective in restraining the lattice parameter change.

The apparent disagreement in the literature on the absolute values of the lattice parameter changes and the $\frac{\Delta c}{c} / \frac{\Delta a}{a}$ ratios is also almost certainly due to this effect. The varying grain size of the materials used by the different workers will have caused variations but in addition the method of measurement is important; parameters obtained using film techniques on powdered specimens will be different from the parameters measured on solid specimens using a diffractometer.

The relatively greater expansion in diameter compared with the expansion in length of specimens from hot-pressed materials A and B is a consequence of the preferred orientation present in these materials. In these specimens the axis of the cylinders was parallel to the hot-pressing direction. J.W.Kelly and K.D.Reeve (A.A.E.C. unpublished) have shown that high density beryllium oxide fabricated by hot pressing has a preferred orientation with the basal planes tending to be parallel to the hot-pressing direction and randomly oriented around it. Although the degree of preferred orientation is slight (1.5 to 2 times random) it is sufficient for the greater expansion of the c parameter compared with the a parameter to result in a greater expansion in the diameter than in the height of the irradiated specimens. A similar effect was also observed in material C after irradiation at pile temperatures. Although cold-pressed and sintered material normally has no preferred orientation, a check on this particular batch of specimens showed that a preferred orientation existed, similar to that in hot-pressed material (J.W.Kelly unpublished). No explanation is offered for this orientation effect.

5.2 Mechanical and Thermal Properties

Insufficient work has been done so far for much comment to be made on the mechanical property changes. As mentioned, Clarke et al. (1961) found a slight increase in strength at low doses and Elston (1962) reported a marked increase in the compressive strength of magnesium oxide after irradiation, suggesting that irradiation hardening occurs in ceramic materials. At higher doses the intergranular stress effects will probably predominate over the irradiation hardening in determining the mechanical properties of beryllium oxide but the actual effect on the tensile strength is complicated by a number of factors and is rather obscure. The bend test results obtained on material A would suggest that no serious deterioration of tensile strength occurs up to doses close to that at which powdering starts to occur. However the results should be treated with some caution because the number of tests was small and the results obtained after irradiation at about 650 °C were anomalous. It will be noted that anomalous X-ray results were also obtained for these specimens whereas those irradiated to a higher dose at the same temperature showed normal behaviour. It is not known whether the loss of strength and the anomalous X-ray results were connected. The results are in contradiction to those of French workers on compressive strength (Section 2.5) but in general agreement with those of the General Electric, Evandale, workers. However owing to different mechanisms of failure a reduction in compressive strength need not be associated with a reduction in modulus of rupture.

The wide scatter in the small number of compressive strength measurements that were made means that the results are of little value. There was some indication that the strength was reduced by irradiation but the reduction was not as great as was observed by Elston and Labbe (1961). It should also be emphasised that from the point of view of using beryllium oxide in a reactor it is the modulus of rupture rather than the compressive strength which is the significant strength property. It is hoped that a more comprehensive programme now under way on modulus of rupture changes on irradiation, will clarify the situation.

A similar situation exists for thermal conductivity in that so far insufficient work has been done. Measurements both overseas and at Lucas Heights have been made at low temperatures but measurements at high temperatures are required to ascertain whether reductions in thermal conductivity will be serious at these temperatures. However, as indicated earlier, it is expected that the reduction in conductivity at high temperatures will be much less than at room temperatures.

5.3 Defect Structure

Many types of defects could exist in beryllium oxide, for example, single beryllium or oxygen interstitials or vacancies, beryllium-oxygen interstitial or vacancy pairs, and larger clusters of various types. The relative stability and mobility of these various types of defects will depend primarily on the relative degree of ionic and covalent bonding and on the relative sizes of the two atoms. Some prelim-

inary theoretical calculations by A.W. Pryor (A.A.E.C. unpublished) have suggested that the bonding in beryllium oxide is predominantly ionic and that oxygen interstitials will be far less mobile than beryllium interstitials and will have a larger effect on the lattice parameters. In an ionic solid, anion–cation vacancy and interstitial pairs will probably be more stable than isolated defects because of their electrical neutrality. Work on alkali halides has suggested that vacancy pairs form readily under irradiation and are more mobile than single vacancies.

In interpreting the data on irradiation effects it is desirable to have information about the total number of defects present in the material and the nature of these defects. Such information as has been obtained from the work described in this report is discussed in this section.

5.3.1 Number of defects

The long wavelength neutron scattering measurements provided figures for the total defect concentration in material irradiated at $<100\,^{\circ}C$ and these figures could be correlated well with the observed lattice expansion.

It is interesting to compare the number of displacements as measured in this manner with values calculated theoretically. Using the simple model due to Kinchin and Pease (1955), the number of displacements per primary knock–on is given by

$$n = \frac{E_i}{2E_d}\left(1 - \frac{E_i}{2E_{max}}\right) ,$$

where:

E_d = minimum energy which must be transferred to cause a displacement,

E_{max} = maximum knock–on energy,

E_i = knock–on energy above which energy is lost primarily by electron excitation and below which energy is lost primarily by elastic collisions,

$= \frac{M_1}{8m} I$ for insulators,

where:

M_1 = mass of moving atom = 12.5 ,

m = mass of electron,

I = lowest electronic excitation energy $\approx$ 5eV,

and therefore:

$$E_i = \frac{12.5 \times 1840 \times 5}{8} \text{ eV} ,$$

$$= 14{,}500 \text{ eV} .$$

Taking E_d = 20 eV, this gives n = 290, whereas the measured value is 15 – 20, that is, an order of magnitude too small. A similar discrepancy has been observed for most other materials and two mechanisms have been proposed to account for it, namely, annealing in thermal spikes (Cottrell 1956) or loss of energy without producing a net increase in displacements by focusing of collisions along close packed directions (Liebfried 1959). However neither process will be as significant in beryllium oxide as in heavier monatomic materials; effects due to thermal spikes will be less than in materials of higher atomic number because knock–on collisions will be further apart; focusing collision effects will be less efficient than in monatomic materials owing to the presence of two atoms of different atomic weights. However these effects will probably occur in beryllium oxide to some extent and, combined with the possibility of some annealing occurring at the irradiation temperatures of $100\,^{\circ}C$, they could explain the discrepancy between the observed and calculated defect concentration.

5.3.2 Nature of defects

The results described in this report do not provide much information about the nature of the defect structure.

Firstly there is no indication of the relative numbers of beryllium and oxygen defects. More beryllium than oxygen primary knock-ons would be produced because of the higher scattering cross section of beryllium. But this would be more than compensated for by the higher scattering cross section of oxygen for knocked on atoms and the net result would probably be roughly equal production rates for the two types of defects; the results do not provide any information on this point.

Secondly there is little concrete evidence for the number and type of point defects. The neutron scattering suggested that a considerable number, perhaps half, of the total number of defects could be present as point defects after irradiation at $<100\,^{\circ}C$.

The electron spin resonance work suggests that there are isolated vacancies present but no quantitative estimates have been made to indicate whether a significant fraction of the total vacancy concentration contributes to the electron spin resonance signal. A.W.Pryor (A.A.E.C. unpublished) has interpreted some preliminary electrical conductivity measurements in terms of conduction by beryllium interstitials. He found that the decrease in resistivity which occurred on irradiation was smaller by a factor of 10^6 than the decrease which would be expected if all the beryllium interstitials which were produced were available as current carriers. He concluded that the majority of the interstitials must be present as neutral beryllium-oxygen pairs or larger clusters. The fact that in the absence of intergranular strain effects the (h,k, o) lines are unbroadened suggests that the $\underset{\sim}{a}$ parameter change in crumbled specimens is due to point defects rather than clusters (see later). The results therefore suggest that point defects are present after irradiation at $<100\,^{\circ}C$ but do not provide information about the nature or relative number of these defects.

Thirdly, however, the results do show conclusively that clusters of defects are present and on the basis of the evidence discussed in the following paragraphs it is suggested that the clusters are planar clusters of interstitial atoms between the basal planes.

The neutron scattering work showed conclusively that defect clusters containing a minimum of fifteen defects per cluster were present but did not provide any information about the nature of the defects making up the clusters. The X-ray line broadening studies showed that, in the absence of intergranular strain effects, there was extensive broadening of the (h, k, l) lines for $l \neq o$. This can only be interpreted in terms of clustered defects as it has been shown that point defects will not give rise to line broadening (Tucker and Senio 1955). It has been suggested by Hickman et al. (1962) that because there is no broadening of the (h, k, o) lines in the absence of intergranular strain effects, the clusters must be extended in the basal planes and have a small dimension perpendicular to the basal plane. These observations are supported by Yakel (see Shields et al. 1962) who made a more detailed analysis of the (h, k, l) line broadening and concluded that it was probably due to planar clusters containing about fifteen defects parallel to the basal planes. The fact that after irradiation at temperatures of $650 - 700\,^{\circ}C$ there is little or no $\underset{\sim}{a}$ parameter change in the absence of intergranular strain effects although there is still a large $\underset{\sim}{c}$ parameter change, together with the anisotropy of the growth under all conditions, shows that the $\underset{\sim}{c}$ parameter change is probably due primarily to the clusters, because isolated defects would be expected to give approximately the same change in both $\underset{\sim}{a}$ and $\underset{\sim}{c}$ parameters. Although vacancy clusters in an ionic solid can cause a lattice expansion (A.W.Pryor A.A.E.C. unpublished), it is considered that only interstitial clusters could produce the large observed effects. A reasonable configuration for a cluster between the basal planes would be one in which a plane containing both beryllium and oxygen atoms at their normal spacing is inserted between the lattice basal planes with the oxygen atoms in the large tetrahedral holes. In this arrangement electrical neutrality is maintained, and the beryllium atoms have beryllium nearest neighbours which could give rise to the observed $\underset{\sim}{c}$ parameter expansion. It can be concluded therefore that the existence of clusters in the basal plane appears to be well established and that it is more likely that these are interstitial rather than vacancy clusters. Further work on line broadening, particularly using single crystals, and further electron microscopy, are required to confirm these propositions.

Clusters could form either as a direct result of the knock-on process or by subsequent diffusion of defects. Seeger (1958) suggested that, in metals such as copper, towards the end of the path of a primary knock-on, collisions occur at very frequent intervals and interstitials leave the atom sites as dynamic crowdions and finally come to rest several hundred Angstroms away. The net result is to produce a region of high concentration of vacancies which could collapse into a vacancy cluster. However, as pointed out

earlier, in a material such as beryllium oxide the knock–on collisions will be further apart than in heavier materials and the focusing of collisions necessary to produce a dynamic crowdion will not be very efficient; nevertheless the process could occur to a limited extent. Both vacancy or interstitial clusters could be produced by diffusion. It is hoped that the electron irradiation studies at present in progress will clarify this point.

5.3.3 Annealing of defects

Studies of the annealing of property changes at elevated temperatures often give useful information about the nature of the defects but in the present work the annealing data did not help a great deal. The results were somewhat self–contradictory and also contradictory to overseas work. The annealing of various property changes in material irradiated to about $1 - 2 \times 10^{20}$ is shown in Figure 11. It can be seen that there were no sharp recovery steps in the annealing of any property and the recovery occurred over a fairly wide temperature range:

(i) The $\underset{\sim}{a}$ parameter annealed in the range 200 – 1000 °C.

(ii) The $\underset{\sim}{c}$ parameter annealed in the range 800 – 1400 °C.

(iii) The long wavelength neutron scattering effect annealed in the range 800 – 1400 °C.

(iv) The thermal resistivity annealed in the range 600 – 1400 °C.

(v) The electron spin resonance signal annealed in the range 400 – 800 °C.

(vi) Broadening of (h, k, l) diffraction lines annealed in the range 1000 – 1400 °C.

Elston (1962) also studied the annealing of the lattice parameters and obtained results in close agreement with our own but Clarke (1962) working on material irradiated to lower doses found a steady annealing of both the $\underset{\sim}{a}$ and $\underset{\sim}{c}$ parameters over the range 200 – 1200 °C. Clarke (1962) attributed this difference to the fact that at lower doses the damage is basically in the form of isolated defects and only at high doses do the more stable clusters become significant. However our own line broadening and long wavelength neutron scattering studies would suggest that the clusters are present in significant quantities even at these lower doses.

The fact that the annealing of all the property changes appears to take place over a fairly wide range of temperatures shows that annealing is not due to simple processes with a unique activation energy. The neutron scattering and X–ray work suggest that the clusters are the more stable defect and do not anneal until 1000 – 1400 °C. Shields et al.(1962) suggest that for irradiation temperatures above 500 °C the damage is predominantly due to isolated defects but our results do not support this hypothesis. As mentioned earlier it is thought that at 600 – 700 °C the clusters cause the majority of the observed property changes and this observation is supported by the (h, k, l) line broadening which is still present, and the stability on annealing of the clusters. The annealing of the $\underset{\sim}{a}$ parameter suggests that isolated defects anneal in the range 200 – 1000 °C but no change in the neutron scattering could be observed until 800 °C; this suggests that the defects diffuse and form a different arrangement rather than become annihilated. Diffusion of isolated defects to form neutral vacancy or interstitial pairs, for instance, could reduce the effect on the lattice parameter without unduly affecting the neutron scattering. The annealing of the thermal conductivity change appears to be a combination of both processes. The annealing of the electron spin resonance signal need not be due to diffusion of defects but could result from loss of electrons and positive holes from the vacancies. However in either case the result is compatible with the above.

Stored energy measurements, which it is hoped will be carried out shortly, should provide useful additional information about the annealing of defects. It is to be expected that most of the stored energy release will occur over the temperature range 800 – 1200 °C. Using the generally accepted value of about 5 eV for the recombination energy of an interstitial–vacancy pair and the measurements of defect concentrations obtained from the neutron scattering work, the total stored energy for irradiation at about 100 °C would be approximately 30 cal/g per 10^{20} nvt with lower values by a factor of 3 to 5 for irradiation at 500 – 1000 °C.

The results of annealing material irradiated at pile temperatures do not enable quantitative prediction of the results at high temperatures. For instance annealing at 600 °C of material irradiated at <100 °C was shown to produce very little change in the $\underset{\sim}{c}$ parameter, even for long annealing periods, but irradiation at 500 – 600 °C resulted in a smaller $\underset{\sim}{c}$ parameter change by a factor of three than for the same dose at

100 °C. Evidently there is an irradiation annealing process which produces this effect. A possible mechanism for this would be annealing in a thermal spike, when the addition of 400 °C to the effect of the thermal spike could result in a much larger volume being raised to a sufficient temperature for a sufficient time for appreciable annealing to occur.

5.4 Effect of Neutron Energy Spectrum on Damage

Throughout the report all neutron doses have been quoted in terms of the flux integrated over the fission neutron spectrum. However the flux spectrum (see Figure 4) in which most of the specimens were irradiated is far from a pure fission spectrum and has a very substantial epithermal neutron component. The minimum energy E_{min} which a neutron must have to cause a displacement in a material is given by:

$$E_{min} = \frac{E_D (1 + A)^2}{4A} ,$$

where E_D = minimum energy which must be imparted to the struck atom to cause a displacement,

and A = atomic weight of the struck atom.

For most materials E_D has been shown to have a value of about 25 eV. A.W.Pryor (A.A.E.C. unpublished) has calculated values of 22 eV and 15 eV for the displacement of beryllium and oxygen atoms respectively in beryllium oxide. Using these values E_{min} is found to be 61 and 68 eV for beryllium and oxygen atoms respectively, so that neutrons right down to these energy levels would produce displacements. Hyder and Kenward (1959) examined this problem theoretically by taking the Kinchin and Pease model for calculating the number of displacements and combining it with calculations of flux spectra in various types of reactors to allow for displacements produced by neutrons of energy down to E_{min}. They concluded that for a D_2O moderated test reactor the damage rate in light materials such as beryllium and carbon in the core will be 30 – 40 times that in a pure fission spectrum and 2 – 3 times that in an H_2O moderated reactor for a given fission neutron dose. These calculations will be in error by a large factor due to simplifications used, particularly the use of the Kinchin and Pease model. For instance, if focusing collisions are important, then knock-ons with energies less than several hundred eV will lose all their energy without producing any additional displacements and this will result in a serious overestimate of the number of displacements produced by neutrons in the lower energy range.

The work described in this report was mainly done in hollow fuel element positions but a 2V-position was used for some of the lower dose irradiations. The flux spectrum in these two positions will be quite different, because the epithermal/fission flux ratio is considerably higher in the 2V-position. However examination of the results on the variation of properties with integrated fission neutron dose shows that there is consistency between results obtained at the lower doses in the 2V-position and at higher doses in the hollow fuel element position (see for instance Figures 5, 6, and 7). The accuracy of measurement of the changes at lower doses was not very great but although there was an indication, particularly from the neutron scattering work, that the damage rate per fission neutron was higher in the 2V-position, the difference was not greater than a factor of 1.5. The integrated fission neutron dose would therefore appear to be a good measure of damage rate in beryllium oxide. Clarke (1962) compared the results of many workers on macroscopic growth and found reasonable agreement on the growth rate per fast neutron. As these results were obtained in reactors with widely differing flux spectra the observation would support the above conclusion. Although Hyder and Kenward's results apparently give a gross overestimate of the effect of the lower energy neutrons, there will undoubtedly be some effect and caution must therefore be exercised when comparing results obtained in different types of test reactors and in extrapolating the results obtained in a test reactor to power reactor systems.

It is hoped that some experiments will be carried out at Lucas Heights on the effect of energy spectrum on the damage rates, to provide more reliable information about this factor.

5.5 Effects of Helium and Tritium Production

As mentioned in Section 5.1 the production of helium and tritium is not the cause of the observed macroscopic and X-ray growth under irradiation. Further it is thought that helium or tritium were not the cause of any of the other property or structural changes observed in the present work. This is in marked contrast to beryllium metal when, at all temperatures, and particularly for temperatures above 500 °C, serious changes occur, particularly in mechanical properties due to the effects of helium production. The

work of Aslanian et al. (1961) (see Section 2.9) suggested that helium diffuses to voids in beryllium oxide at temperatures as low as 600 °C but, as they did not attempt to quantify their results, it is not known whether they were seeing a significant proportion of the helium. The electron microscope observations of Shields et al. (1962) and Frisby et al. (1959) would suggest that accumulation of helium into bubbles may occur at irradiation temperatures around 1000 °C but the situation is complicated by the void formation observed in unirradiated material. If helium bubble formation occurred primarily at grain boundaries it could produce deleterious effects on the mechanical properties of the material but would not be expected to produce density changes of such significance. However further studies, particularly of specimens irradiated in the region 1000 – 1200 °C, are required to elucidate this point.

The results reported by Shields et al. (1962) show that at least for irradiation temperatures above 400 °C most of the tritium will diffuse out even from high density beryllium oxide. This behaviour is not unexpected but in a reactor moderated by beryllium oxide it could result in high tritium activity in the coolant circuits. In a 300 MW(e) reactor containing approximately 100 m^3 of beryllium oxide for instance, approximately 10^7 curies of tritium per year would be produced.

5.6 Assessment of Beryllium Oxide as a Reactor Material

The main requirements that must be met by beryllium oxide if it is to be successfully used as a moderator or fuel diluent in a high temperature gas–cooled reactor are that any reductions in mechanical strength or thermal conductivity should not be so large as to unduly affect the resistance of the material to thermal stress or thermal shock. Although no results have been obtained to date, it is not expected that the other properties which govern the thermal stress behaviour of the material, namely the coefficient of expansion, Young's Modulus, Poisson's ratio, or specific heat will be significantly affected by irradiation. It is also important that dimension changes be kept to a minimum and that there should be no significant changes in open porosity which could result in increased escape of fission products to the coolant circuits.

Early results on coarse–grained hot–pressed material were somewhat discouraging because they showed that crumbling and complete loss of strength occurred at relatively low doses and that very large changes in the room temperature conductivity occurred. Although much more work has to be done, the results described in this report give grounds for optimism that the above requirements can be met. The points of particular significance in this respect are:

(i) The superiority of very fine grained material over coarse–grained material in withstanding the crumbling due to the anisotropic growth processes.

(ii) The much reduced rate of damage at temperatures of 500 – 700 °C compared with that at about 100 °C.

(iii) The tentative suggestion that the thermal conductivity in the range 500 – 1000 °C will not be affected by irradiation to nearly the same amount as it is at 100 °C.

(iv) The tentative result that the modulus of rupture is not markedly reduced until doses very close to that at which crumbling occurs are experienced.

(v) The negligible changes in open porosity in fine–grained material.

(vi) The possibility of the relief of the intergranular stresses by creep, particularly at temperatures approaching 1000 °C, or at lower temperatures in material containing additions which form a plastic grain boundary network.

Combining these facts it would appear that the fine–grained material could withstand doses of at least 1.5×10^{20} nvt at elevated temperatures without cracking or crumbling. Further work is required to confirm this and to determine whether the material will withstand higher doses. The possibility always exists of removing the beryllium oxide from the reactor and annealing out the damage by heating to 1200 – 1400 °C or even of heating it in situ to these temperatures, particularly in the case of a moderator containing no fuel additions.

The dimension changes, particularly in fine–grained material, will probably be of the order of 1 to 2 per cent. for doses of about 10^{21} nvt at 500 – 1000 °C but these should not be too excessive to be allowed for in the reactor design. Porosity changes would appear to be very small in the fine–grained material so increased rates of fission product escape should not occur. As mentioned earlier the buildup of stored energy in beryllium oxide could be of the same order as in graphite and could amount to about

100 cal/g for irradiation to around 10^{21} nvt at 500 – 1000 °C. As the main release of stored energy will probably occur in the temperature region 800 – 1200 °C, that is, near the likely top operating temperatures in an H.T.G.C. reactor, careful consideration will have to be given to this in the reactor design.

6. SUMMARY AND CONCLUSIONS

1. Under neutron irradiation the beryllium oxide lattice expands anisotropically; the expansion in the $\underset{\sim}{c}$ direction is considerably greater than the expansion in the $\underset{\sim}{a}$ direction.

2. This anisotropic growth results in crumbling of the material at a dose which depends primarily on the irradiation temperature and the grain size of the material rather than on density. Fine-grained material withstands considerably higher doses than coarse-grained material before microcracking and powdering occurs.

3. Macroscopic growth of polycrystalline material agrees closely with the theoretical growth as calculated from the lattice parameters at low doses but at higher doses ($> 1 \times 10^{20}$ nvt) exceeds the theoretical growth. This is primarily due to cracking and void formation resulting from the anisotropic growth process.

4. The intergranular strains resulting from the anisotropic growth process affect the lattice parameters and result in broadening of the (h, k, o) reflections. The measured values of the lattice parameters at any dose depend on the grain size of the material, on whether the material has crumbled, and on the method of measurement.

5. There is some evidence that the bend strength does not fall off significantly until close to the dose at which crumbling and complete loss of strength occurs.

6. Large changes in the thermal conductivity occur at room temperatures but analysis of the results suggests that at temperatures in the range 500 – 1000 °C the changes will be much smaller.

7. In material irradiated at 100 °C the majority of the property changes anneal in the range 800 – 1400 °C although some properties ($\underset{\sim}{a}$ parameter and electron spin resonance signal) anneal at lower temperatures.

8. Irradiation at 500 – 700 °C results in property changes which are a factor of 3 to 5 smaller than for the same dose at 100 °C. This would not be expected from the annealing data and is evidently the result of an irradiation annealing process.

9. Measurements of defect concentration by long wavelength neutron scattering techniques show that the lattice expansion is a direct result of lattice defects, each defect pair resulting in an expansion of approximately one atomic volume.

10. It is considered that none of the property changes reported are due to helium and tritium produced by transmutation reactions but the effects of helium may become important for irradiation temperatures around 1000 °C and above.

11. The long wavelength neutron scattering results and X-ray line-broadening studies show that planar clusters of defects in the basal planes are present for all irradiation temperatures and doses investigated. It is suggested that these clusters are the prime cause of the greater expansion in the $\underset{\sim}{c}$ direction compared with the $\underset{\sim}{a}$ direction. Little further can be concluded from the available data as to the nature of the defect structure.

12. Although much more work has to be done, particularly on mechanical property changes and thermal conductivity changes at high temperatures, some confidence can now be expressed that fine-grained beryllium oxide can be used as a moderator or fuel matrix material at temperatures of 500 – 1000 °C up to doses of at least 1.5×10^{21} nvt.

7. ACKNOWLEDGMENTS

The work described in this report is the result of a cooperative effort between many members of the Research Establishment; the majority of whose contributions have been acknowledged in the text. Many of the ideas expressed are the result of discussions with members of the Materials Division particularly Dr. A.W. Pryor, Dr. K.D. Reeve, Mr. T.M. Sabine, Dr. R. Smith, and Mr. D.G. Walker. Particular

acknowledgment is given to Dr. K.D.Reeve and the staff of the Ceramics Group whose care and close control in the fabrication of specimens contributed much to the success of the investigations.

Acknowledgment is also due to Mr. K.F.Alder for his interest and encouragement, particularly in the early stages of the work; to members of the Rig Group and Reactor Operations Section for carrying out the irradiation of the specimens; to the Hot Cells Group for the disassembly of the rigs and some preliminary examination; to the Analytical Chemistry Section and Reactor Physics Division for assistance with flux monitoring; and to many members of the Materials Physics Section who contributed to the work in various ways.

8. REFERENCES

Aslanian, J., Caillat, R., Salisse, M., and Weil, L. (1961). – Comptes Rendus 253: 1032.

Bacon, G.E., and Wilson, S.A., (1955). – Acta Cryst. 8: 844.

Bisson, A., and Frisby, H. (1961). – J. Nucl. Mat. 4: 133.

Bowen, D.H., Wilks, R.S., and Clarke, F.J.P. (1962). – J. Nucl. Mat. 6: 148.

Clarke, F.J.P. (1962). – AERE R–3971.

Clarke, F.J.P., Tappin, G., and Ghosh, T.K.(1961). – J. Nucl. Mat. 4: 125.

Clarke, F.J.P., and Williams, J. (1961). – J. Nucl. Mat. 4: 121.

Cottrell, A.H. (1956). – Met. Reviews 1: 479.

Elston, J., and Caillat, R. (1958). – 2nd U.N. Conference Proceedings 5: 345.

Elston, J. (1962). – Paper presented at I.A.E.A. Conference on Irradiation Damage, Venice (No. DM–1182)

Elston, J., and Labbe, C. (1961). – J. Nucl. Mat. 4: 143.

Frisby, H., Bisson, A., and Caillat, R. (1959). – J. Nucl. Mat. 1: 106.

Hickman, B.S. (1962). – AAEC/TM139.

Hickman, B.S., Sabine, T.M., and Coyle, R.A. (1962). – J. Nucl. Mat. 6: 190.

Hyder, H.R., and Kenward, C.J. (1959). – AERE R–2886.

James, R.W., (1958). – "The Optical Principles of the Diffraction of X–Rays", G.Bell and Sons Ltd., London.

Kinchin, G.H., and Pease, R.S. (1955). – Repts. Prog. in Phys. 18: (1).

Lang, G.B. (1962). – AAEC/TM132.

Liebfried, G. (1959). – J. Appl. Phys. 30: 1388.

McGill, R.C., and Smith, J.A.G. (1959). – AERE R–3019.

Reeve, K.D., and Ramm, E.J. (1961a). – AAEC/TM103.

Reeve, K.D., and Ramm, E.J. (1961b). – AAEC/E80.

Sabine, T.M., Pryor, A.W., and Hickman, B.S. (1962). – AAEC/TM140. To be published in Phil. Mag.

Seeger, A. (1958). – Proc. of 2nd Int. Conf. on Atomic Energy 6: 250.

Shields, R.P., Lee, J., and Browning, W. (1962). – ORNL 3164.

Tobin, M.J. (1962). – General Atomic Report, GA-2648.

Troup, G.J., and Thyer, J.R.W. (1962). – Proc. Phys. Soc. 79 : 409.

Tucker, C.W., and Senio, P. (1955). – Phys. Rev. 99 : 1777.

TABLE 1

INTEGRATED FISSION NEUTRON FLUXES AND HELIUM CONCENTRATIONS FOR VARIOUS U/Be ATOM RATIOS AND BURN-UPS IN AN H.T.G.C. REACTOR SYSTEM

U/Be Atom Ratio	100 Per Cent. Burn-up		300 Per Cent. Burn-up	
	Integrated Fission Neutron Flux nvt	Helium Concentration cm^3 at NTP/cm^3	Integrated Fission Neutron Flux nvt	Helium Concentration cm^3 at NTP/cm^3
1:500	4.8×10^{21}	3.1	1.4×10^{22}	9.3
1:1000	2.4×10^{21}	1.6	7×10^{21}	4.7
1:2000	1.2×10^{21}	0.8	3.6×10^{21}	2.3
1:4000	6×10^{20}	0.4	1.8×10^{21}	1.2
1:8000	3×10^{20}	0.2	9×10^{20}	0.6

Note: Burn-up is here defined as the percentage ratio of the number of fissions to the number of uranium atoms originally present.

TABLE 2

SUMMARY OF MATERIALS USED IN THE INVESTIGATION

The reference code in column 1 is used throughout the text for referring to the various materials

Code	Starting Material	Fabrication Method	Density % of theoretical	Grain Size Microns
A	Pechiney	Hot Pressing	96–98	10–20
B	Berylco No. 1	Hot Pressing	>99.5	25–30
C	Brush UOX (pre-ground)	Cold Pressing and sintering	97–98	7.5–15
D	,,	,,	90–93	$<2\mu$
E	,,	,,	94–97	$<3\mu$
F	Brush UOX	,,	95–96	$20-30\mu$
G	,,	,,	72–75	$<1\mu$

TABLE 3

DETAILS OF DOSE AND TEMPERATURE AT WHICH SPECIMENS WERE IRRADIATED IN THE VARIOUS RIGS

Rig No.	Position	Number of Specimens	Size of Specimens inches	Material	Irradiation Temperature	Irradiation Dose nvt
X4	H.F.E. C–3	8	¾" ϕ x ¾"	A	75–100 °C	1.8×10^{20}
		4	0.15" x 0.23" x 0.97"	A	75–100 °C	9×10^{19}
		13	0.3" ϕ x 0.6"	A	75–125 °C	1.2×10^{20}
X5	H.F.E. C–1	4	0.15" x 0.23" x 0.97"	A	500–520 °C	1.2×10^{20}
		4	"	A	600–620 °C	1.0×10^{20}
		4	"	A	640–660 °C	1.5×10^{20}
		6	0.3" ϕ x 0.6"	A	500–520 °C	1.2×10^{20}
		6	"	A	610–630 °C	1.1×10^{20}
		6	"	A	650–670 °C	1.1×10^{20}
X22	2V–3	8	¾" ϕ x ¾"	A	75–100 °C	2.5×10^{19}
		4	0.15" x 0.23" x 0.97"	A	"	1.2×10^{19}
		13	0.3" ϕ x 0.6"	A	"	2×10^{19}
X38	2V–3	8	¾" ϕ x ¾"	A	70–80 °C	5.8×10^{19}
		4	0.15" x 0.23" x 0.97"	A	"	2.5×10^{19}
		13	0.3" ϕ x 0.6"	A	"	4.0×10^{19}
X39	H.F.E. C–3	8	¾" ϕ x ¾"	A	70–80 °C	6.8×10^{20}
		4	0.15" x 0.23" x 0.97"	A	"	3.5×10^{20}
		13	0.3" ϕ x 0.6"	A	"	4.5×10^{20}
X73	H.F.E. C–1	4	0.3" ϕ x 0.6"	A	510–540 °C	6×10^{20}
		4	"	A	580–600 °C	5×10^{20}
		4	"	A	650–690 °C	7×10^{20}
		4	0.3" ϕ x 0.6"	F	510–540 °C	6×10^{20}
		4	"	F	580–600 °C	5×10^{20}
		4	"	F	650–690 °C	7×10^{20}
		4	"	G	510–540 °C	6×10^{20}
		4	"	G	580–600 °C	5×10^{20}
		4	"	G	650–690 °C	7×10^{20}

(continued)

TABLE 3 (continued)

Rig No.	Position	Number of Specimens	Size of Specimens inches	Material	Irradiation Temperature	Irradiation Dose nvt
X75/4	H.F.E. C–3	2	0.4" ϕ x 0.6"	A	50–100 °C	3 x 10^{20}
		2	"	B	"	"
		4	"	C	"	"
		4	"	D	"	"
		4	"	E	"	"
X75/5	H.F.E. C–3	2	0.4" ϕ x 0.6"	A	50–100 °C	5 x 10^{20}
		2	"	B	"	"
		4	"	C	"	"
		4	"	D	"	"
		4	"	E	"	"

TABLE 4

DIMENSION CHANGES ON IRRADIATION

Irradiation Dose	Irradiation Temperature °C	Material	Number of Samples	Diameter Change %		Length Change %		Volume Change %	Remarks
				Mean	r.m.s.	Mean	r.m.s.		
2×10^{19}	75–100	A	8	0.03	±0.01	.04	±0.02	0.1	
4.5×10^{19}	75–100	"	8	0.05	±0.02	0.05	±0.02	0.15	
1.2×10^{20}	75–125	"	8	0.10	±0.04	0.15	±0.05	0.35	
1.8×10^{20}	75–125	"	8	0.21	±0.04	0.19	±0.02	0.6	
4×10^{20}	75–100	"	4	0.65	±0.10	0.6	±0.07	1.9	Material cracked and crumbled under irradiation
6.5×10^{20}	75–100	"	4	–	–	0.9	±0.1	–	
3×10^{20}	75–100	"	2	0.72	±0.05	0.54	±0.01	2.0	
		B	2	0.72	–	0.53	±0.01	2.0	
		C	4	0.30	±0.02	0.20	±0.02	0.80	
		D	4	0.22	±0.04	0.18	±0.02	0.62	
		E	4	0.19	±0.02	0.13	±0.01	0.51	
5×10^{20}	75–100	A	2	1.72	±0.20	1.22	±0.08	4.6	
		B	2	1.37	±0.05	–	–	–	Material crumbled under irradiation
		C	4	1.07	±0.05	0.66	±0.04	2.8	
		D	4	0.79	±0.04	0.78	±0.08	2.4	
		E	4	0.65	±0.02	0.56	±0.02	1.8	
1.5×10^{20}	650–670	A	6	0.06	±0.02	.03	±0.01	0.15	
1.1×10^{20}	610–630	"	6	0.05	±0.02	0.035	±0.01	0.14	
1.2×10^{20}	500–520	"	6	0.1	±0.02	0.05	±0.02	0.2	
7×10^{20}	650–690	"	4	0.53	±0.02	0.22	±0.05	1.3	
		F	4	0.21	±0.04	0.13	±0.02	0.55	
		G	4	0.31	±0.04	0.25	±0.04	0.87	
5×10^{20}	580–600	A	4	0.60	±0.03	0.32	±0.04	1.5	
		F	4	0.21	±0.03	0.15	±0.03	0.56	
		G	4	0.17	±0.07	0.22	±0.04	0.58	
6×10^{20}	510–540	A	4	0.65	±0.07	0.37	±0.03	1.7	
		F	4	0.28	±0.03	0.23	±0.03	0.79	
		G	4	0.18	±0.03	0.20	±0.04	0.56	

TABLE 5

POROSITY OF VARIOUS SPECIMENS BEFORE AND AFTER IRRADIATION

Material	Irradiation Dose	Irradiation Temperature °C	Pre–Irradiation Porosity			Post Irradiation Porosity			Change		
			Total Porosity %	Open Porosity %	Closed Porosity %	Total Porosity %	Open Porosity %	Closed Porosity %	Total Porosity %	Open Porosity %	Closed Porosity %
A	3×10^{20}	75–100	2.0	0.7	1.3	3.2	2.6	0.6	1.2	1.9	−0.7
B	3×10^{20}	75–100	<0.5	<0.5	<0.5	3.0	2.9	0.1	3.0	2.9	–
C	3×10^{20}	75–100	3.2	0.6	2.6	3.9	0.9	3.0	0.7	0.3	0.4
D	3×10^{20}	75–100	10.0	7.9	2.1	9.8	7.5	2.3	−0.2	−0.4	0.2
E	3×10^{20}	75–100	4.1	0.6	3.5	4.3	0.65	3.65	0.2	–	0.2
C	5×10^{20}	75–100	3.4	0.7	2.7	4.5	2.4	3.0	2.0	1.7	0.3
D	5×10^{20}	75–100	11.6	10.0	1.6	12.7	8.5	4.2	1.1	−1.5	2.6
E	5×10^{20}	75–100	4.0	0.6	3.4	5.1	0.8	4.3	1.1	0.2	0.9
A	6×10^{20}	510–540	1.3	0.3	1.0	2.5	2.0	0.5	1.2	1.7	−0.5
F	6×10^{20}	510–540	4.2	0.8	3.4	4.2	2.7	1.5	–	1.9	−1.9
G	6×10^{20}	510–540	27	27	0	28	27	1.0	–	–	–
A	5×10^{20}	580–600	1.5	0.2	1.3	2.4	2.0	0.4	0.9	1.8	−0.9
F	5×10^{20}		4.0	0.7	3.3	3.8	1.7	2.1	−0.2	1.0	−1.2
G	5×10^{20}		27.5	27.5		28	28	–	–	–	–
A	7×10^{20}	650–690	1.5	0.2	1.3	2.2	1.8	0.4	0.7	1.6	−0.9
F	7×10^{20}		4.3	1.4	2.9	4.2	2.5	17	−0.1	+ 1.1	−1.2
G	7×10^{20}		27	27	–	28	28	–	–	–	–

TABLE 6

X-RAY LATTICE PARAMETER CHANGES AND LINE BROADENING

Material	Dose	Irradiation Temperature °C	$\frac{\Delta c}{c}$ %	$\frac{\Delta a}{a}$ %	Broadening 300 line (Degrees of θ)	$\frac{\Delta c}{c} / \frac{\Delta a}{a}$	X-Ray Volume Change	Macroscopic Volume Change	Remarks
A	1.2×10^{19}	75–100	0.04 ±0.02	0.008 ±0.001	0.04	5	0.056	0.05	
A	2.5×10^{19}	75–100	0.09 ±0.02	0.018 ±0.001	0.07	5	0.125	0.1	
A	9×10^{19}	75–100	0.19 ±0.02	0.056 ±0.001	0.20	3.5	0.30	0.3	
A	9×10^{19}	75–100	0.31 ±0.02	0.035 ±0.002	–	9	0.38	–	Results on crushed specimen
A	3×10^{20}	75–100	0.71 ±0.05	0.073 ±0.002	nil	13	0.81	2.0	
B	3×10^{20}	75–100	0.69 ±0.05	0.070 ±0.002	nil	10	0.83	2.0	
C	3×10^{20}	75–100	0.46 ±0.05	0.11 ±0.01	0.55	4	0.68	0.8	
D	3×10^{20}	75–100	0.25 ±0.05	0.065 ±0.005	0.22	4	0.38	0.6	
E	3×10^{20}	75–100	0.23 ±0.05	0.075 ±0.005	0.30	3	0.38	0.5	
A	3.5×10^{20}	75–100	1.0 ±0.2	0.086 ±0.002	nil	16	1.57	1.9	Specimen cracked and friable after irradiation
C	5×10^{20}	75–100	Not measured	0.11 ±0.02	0.20	–	–	2.8	
D	5×10^{20}	75–100	due to excess-	0.12 ±0.02	0.71	–	–	2.4	
E	5×10^{20}	75–100	ive broadening	0.14 ±0.02	0.92	–	–	1.8	
A	1.2×10^{20}	500–520	0.065 ±0.02	0.026 ±0.002	0.10	3	.12	0.2	
A	6×10^{20}	500–530	0.52 ±0.05	0.010 ±0.002	nil	50	.54	1.7	
F	6×10^{20}	500–530	0.48 ±0.05	0.019 ±0.005	0.38	15	0.52	0.79	
G	6×10^{20}	500–530	0.37 ±0.05	0.018 ±0.005	0.32	21	0.41	0.56	
A	1.1×10^{20}	600–620	0.07 ±0.02	0.027 ±0.002	0.10	3	0.12	0.15	
A	5×10^{20}	560–600	0.29 ±0.05	0.010 ±0.002	0.08	30	0.31	1.5	Results from two specimens (795, 798)
			0.43 ±0.05	0.000 ±0.002	0.03		0.43	1.5	Results from one specimen (796)
F	5×10^{20}	560–600	0.23 ±0.05	0.015 ±0.005	0.25	15	0.26	0.56	
G	5×10^{20}	560–600	0.27 ±0.05	0.015 ±0.005	0.22	17	0.30	0.58	
A	1.5×10^{20}	640–660	0.02–0.08 –	0.004–0.026 –	0.2–0.4		–	0.14	Wide variation between specimens
A	7×10^{20}	640–690	0.27 ±0.05	zero ±0.002	nil		0.27	1.3	
F	7×10^{20}	640–690	0.25 ±0.05	0.019 ±0.004	0.38	13	0.29	0.55	
G	7×10^{20}	640–690	0.23 ±0.05	0.014 ±0.005	0.25	16	0.26	0.87	

TABLE 7

RESULTS OF MODULUS OF RUPTURE MEASUREMENTS ON MATERIAL A IRRADIATED TO VARIOUS CONDITIONS

For the four specimens irradiated to 1.5×10^{20} at 640 – 660 °C each result has been quoted separately owing to the very wide scatter.

Irradiation Dose	Irradiation Temperature °C	No. of Specimens	Modulus of Rupture p.s.i. (mean)	Range p.s.i.
1.2×10^{19}	75 – 100	4	30,400	29,800 – 30,600
2.5×10^{19}	75 – 100	4	24,400	21,000 – 27,200
9×10^{19}	75 – 100	4	28,700	25,400 – 31,200
1.2×10^{20}	500 – 520	4	27,200	24,200 – 30,100
1×10^{20}	600 – 620	4	25,000	22,800 – 26,200
1.5×10^{20}	640 – 660	–	10,450	– –
			27,150	
	– –		13,600	
			18,800	
Unirradiated	– –	13	27,300	26,100 – 29,250
Unirradiated	Heat Treated at 500 – 660	8	25,800	22,800 – 32,800

TABLE 8

RESULTS OF COMPRESSIVE STRENGTH MEASUREMENTS ON MATERIAL A IRRADIATED TO VARIOUS CONDITIONS

Dose	Irradiation Temperature °C	No. of Specimens	Compressive Strength p.s.i.(mean)	Range p.s.i.
1.2×10^{20}	500 – 520	3	160,000	120 – 212,000
1.1×10^{20}	600 – 620	3	119,000	102 – 145,000
1.5×10^{20}	640 – 660	2	204,000	197 – 212,000
2×10^{19}	75 – 100	5	193,000	145 – 256,000
4.5×10^{19}	75 – 100	7	174,000	112 – 212,000
Unirradiated	–	6	205,000	145 – 260,000

TABLE 9

DEFECT CONCENTRATIONS VERSUS NEUTRON DOSES FOR MATERIAL A AS ESTIMATED BY NEUTRON SCATTERING METHODS

Rig Number	Fission Neutron Dose nvt	Primary Collisions per cm^3	Atoms Displaced per cm^3	Atoms Displaced per Primary Collision
X–39	6.8×10^{20}	2.4×10^{20}	$41 \times 10^{20} \pm 5\%$	16 – 18
X–4	1.8×10^{20}	6.4×10^{19}	$8.0 \times 10^{20} \pm 10\%$	11 – 14
X–38	5.8×10^{19}	2.1×10^{19}	$4.8 \times 10^{20} \pm 20\%$	18 – 26
X–22	2.5×10^{19}	0.9×10^{19}	$1 \times 10^{20} \pm 100\%$	5 – 20

TABLE 10

THERMAL CONDUCTIVITY AT 45 °C OF IRRADIATED AND UNIRRADIATED MATERIAL

The quoted results are generally the mean for two specimens and are considered to be accurate to ± 1%. These results are taken from Cooper et al.(unpublished) and Heuer et al. (unpublished).

Irradiation Dose	Irradiation Temperature °C	Material	Thermal Conductivity cal $sec^{-1} cm^{-1} (deg.C)^{-1}$	Remarks
2×10^{19}	70 – 80	A	0.390	Normal temp. dependence
1.2×10^{20}	130 – 140	A	0.168	Temp. independent from 0–90 °C
4.5×10^{20}	70 – 80	A	0.033	,, ,,
1.2×10^{20}	500 – 520	A	0.0295	,, ,,
1.1×10^{20}	610 – 630	A	0.368	Normal temp. dependence
1.5×10^{20}	650 – 670	A	0.365	,, ,,
5×10^{20}	580 – 600	A	0.093	
7×10^{20}	650 – 690	A	0.195 0.155	Density 2.97 Density 2.93
Unirradiated	–	A	0.500 0.479	Density 2.97 Density 2.90
6×10^{20}	510 – 540	F	0.145	
Unirradiated	–	F	0.440	Density 2.88
6×10^{20}	510 – 540	G	0.111	
Unirradiated	–	G	0.173	

TABLE 11

ESTIMATED THERMAL CONDUCTIVITY OF HIGH DENSITY BERYLLIUM OXIDE IN A REACTOR – cal sec^{-1} cm^{-1} $(deg. C)^{-1}$

	600 °C	800 °C	1000 °C
Unirradiated	0.115	0.064	0.050
2×10^{20} nvt	0.095	0.062	0.050
8×10^{20} nvt	0.066	0.052	0.048

TABLE 12

COMPARISON OF DEFECT CONCENTRATION AND LATTICE EXPANSION FOR MATERIAL A

a = atomic volume

Neutron Dose nvt	Atoms Displaced %	Volume Expansion %	Volume Expansion for Defect Pair
6.8×10^{20}	2.6 ± 0.1	3.0 ± 0.4	1.0 – 1.3 a
1.8×10^{20}	0.51 ± 0.05	0.60 ± 0.05	1.0 – 1.4 a
5.8×10^{19}	0.36 ± 0.05	0.27 ± 0.05	0.55 – 1.0 a
2.8×10^{19}	0.07 ± 0.07	0.15 ± 0.05	0 – 3 a

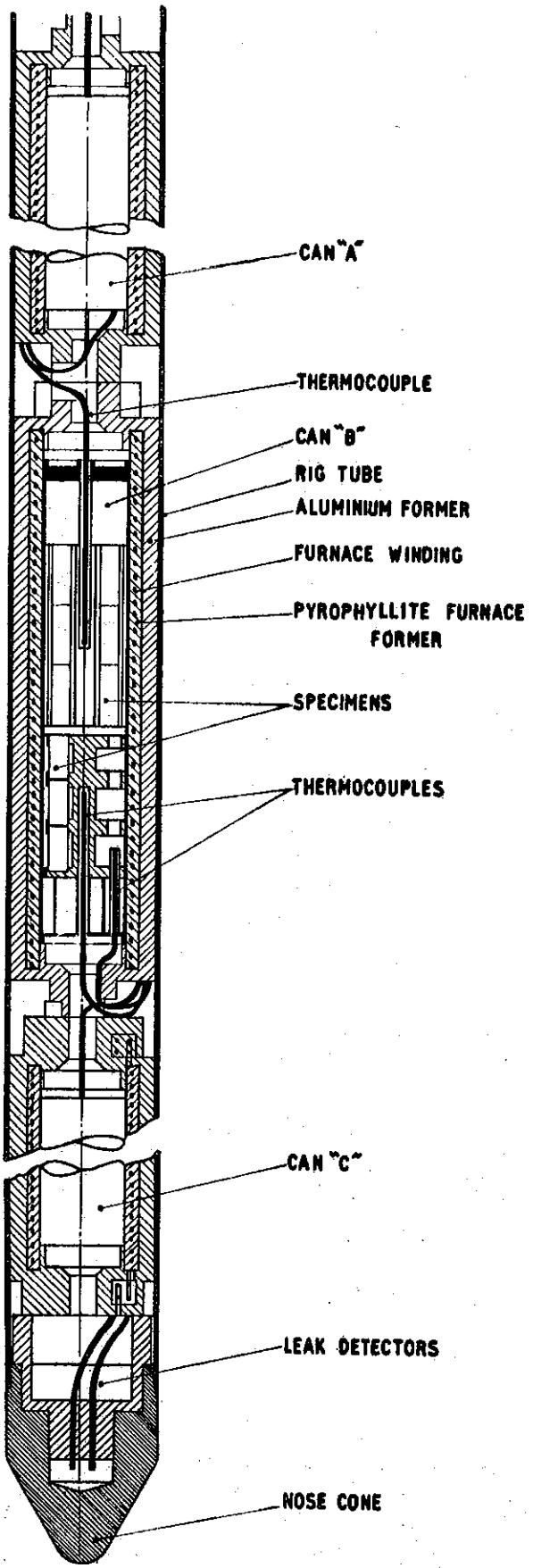

FIGURE 1.
EXPERIMENT ASSEMBLY FOR HIGH TEMPERATURE IRRADIATION.

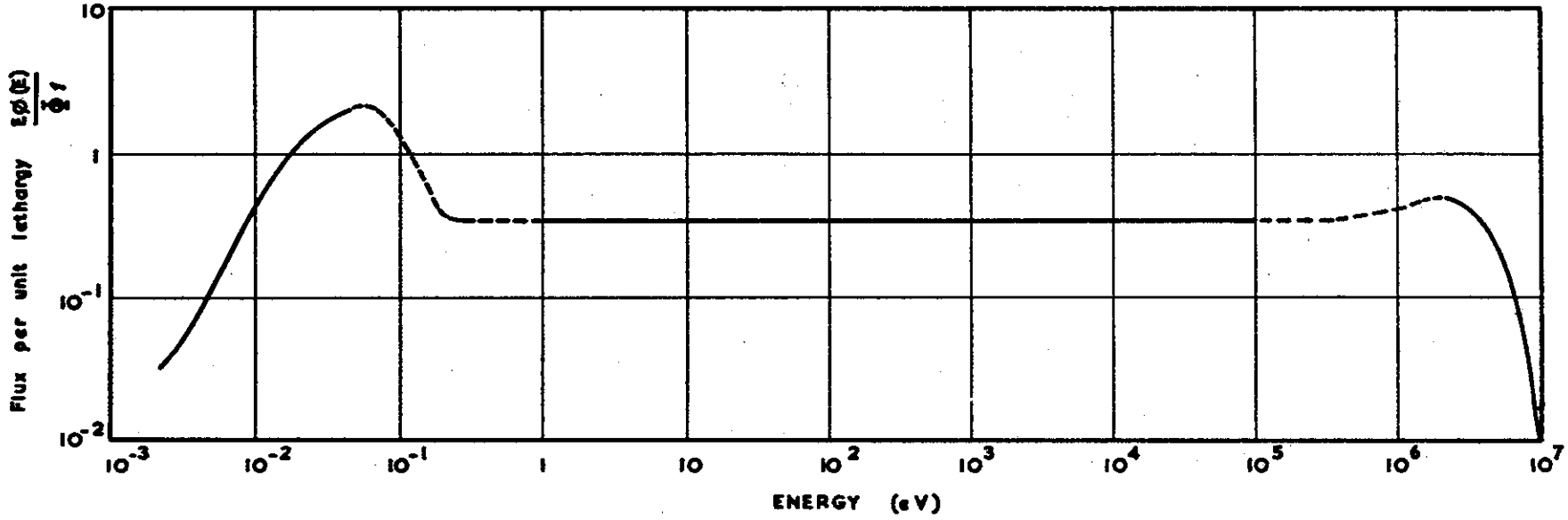

FIGURE 2.

GRAPH OF NEUTRON SPECTRUM IN C-3 HOLLOW FUEL ELEMENT POSITION IN HIFAR

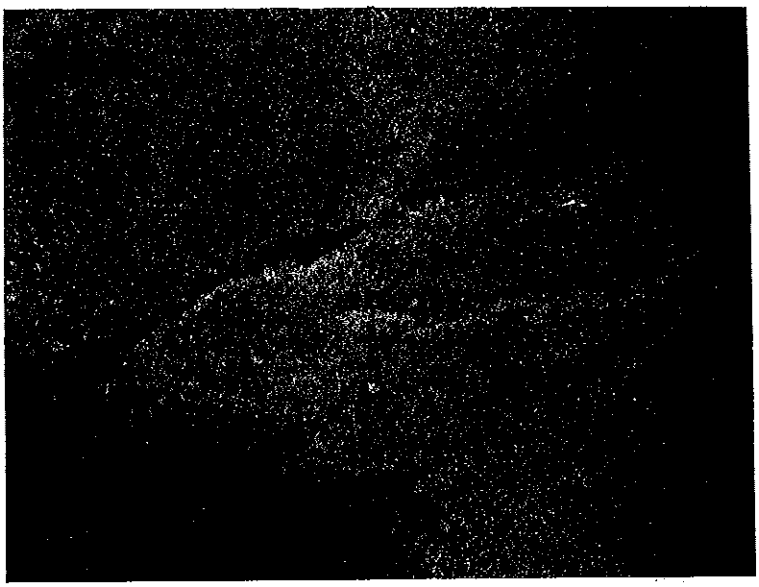

X 20

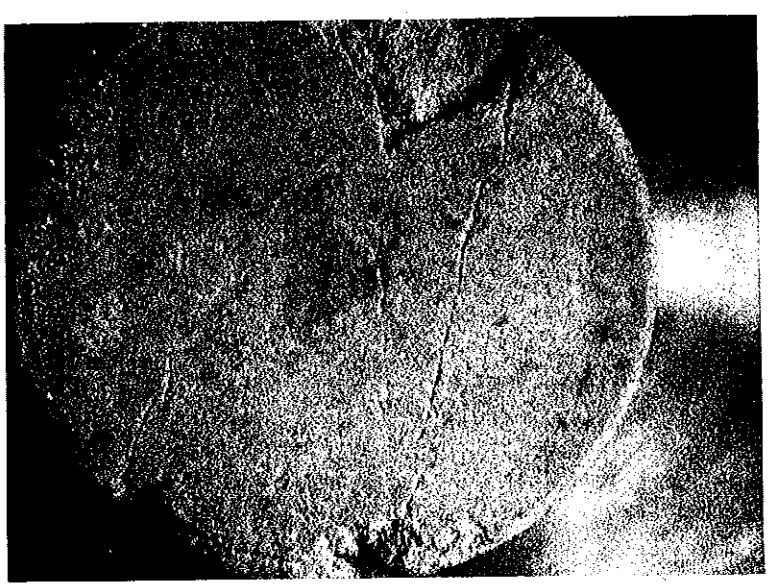

X 4.4

FIGURE 3 PHOTOGRAPHS OF MATERIAL A IRRADIATED TO 6×10^{20} nvt AT $< 100\,^{\circ}C$ SHOWING CRACKING AND CRUMBLING

(a) X 4.4

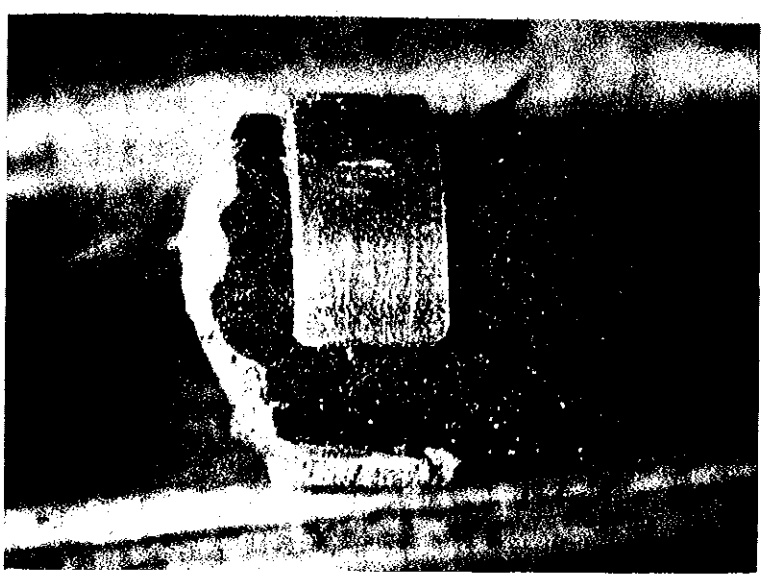

(b) X 4.4

FIGURE 4 PHOTOGRAPHS OF MATERIAL B IRRADIATED TO 5 x 10^{20} nvt AT $<100\,^{\circ}C$ SHOWING CRUMBLING

(a) Comparison of material B with cold–pressed and sintered material C (on right)

(b) Side view of material B

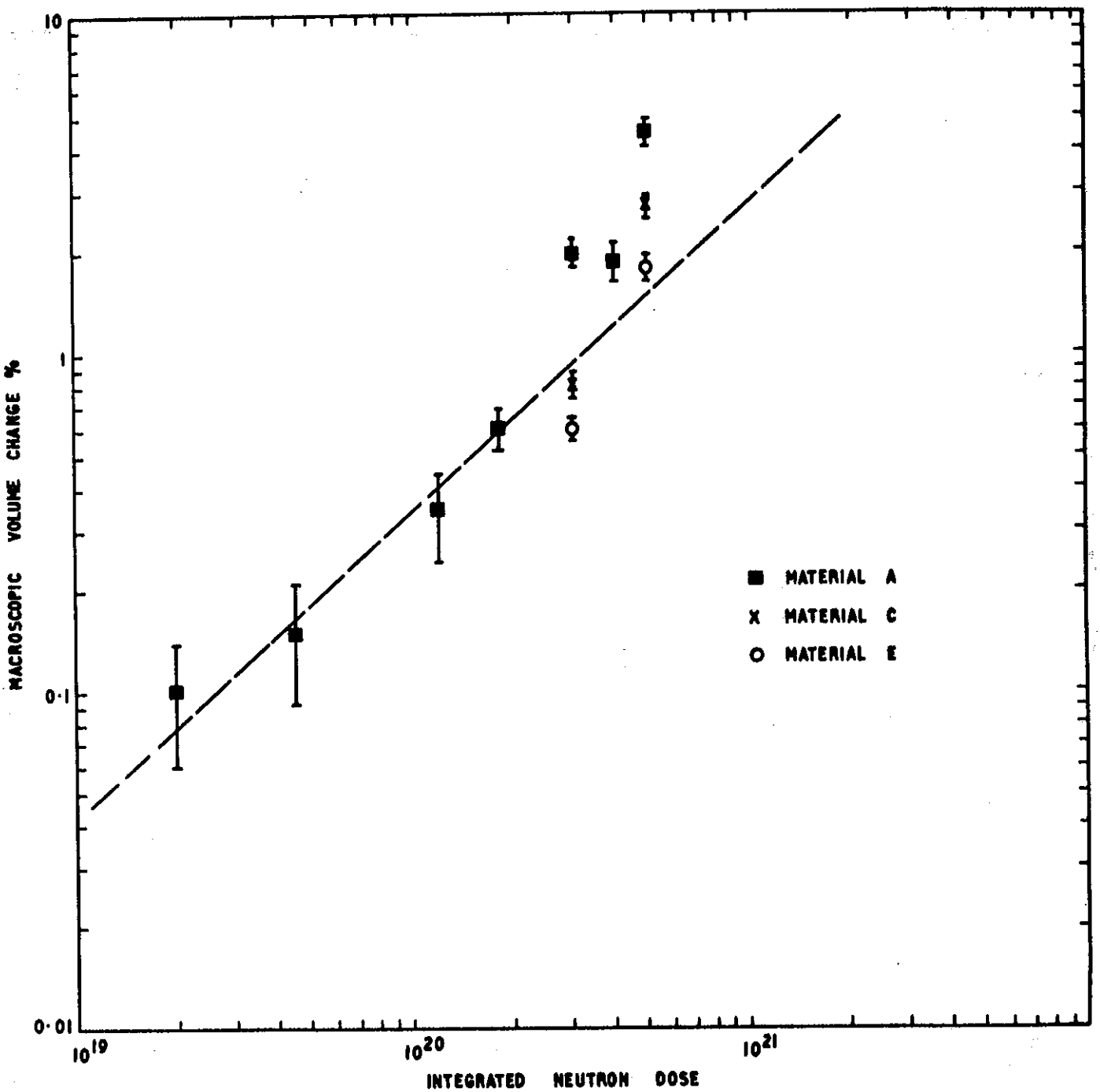

FIGURE 5.
MACROSCOPIC GROWTH VERSUS NEUTRON DOSE FOR MATERIAL IRRADIATED AT $< 100^{\circ}C$

The broken line is the suggested growth of coarse-grained material in the absence of microcracking.

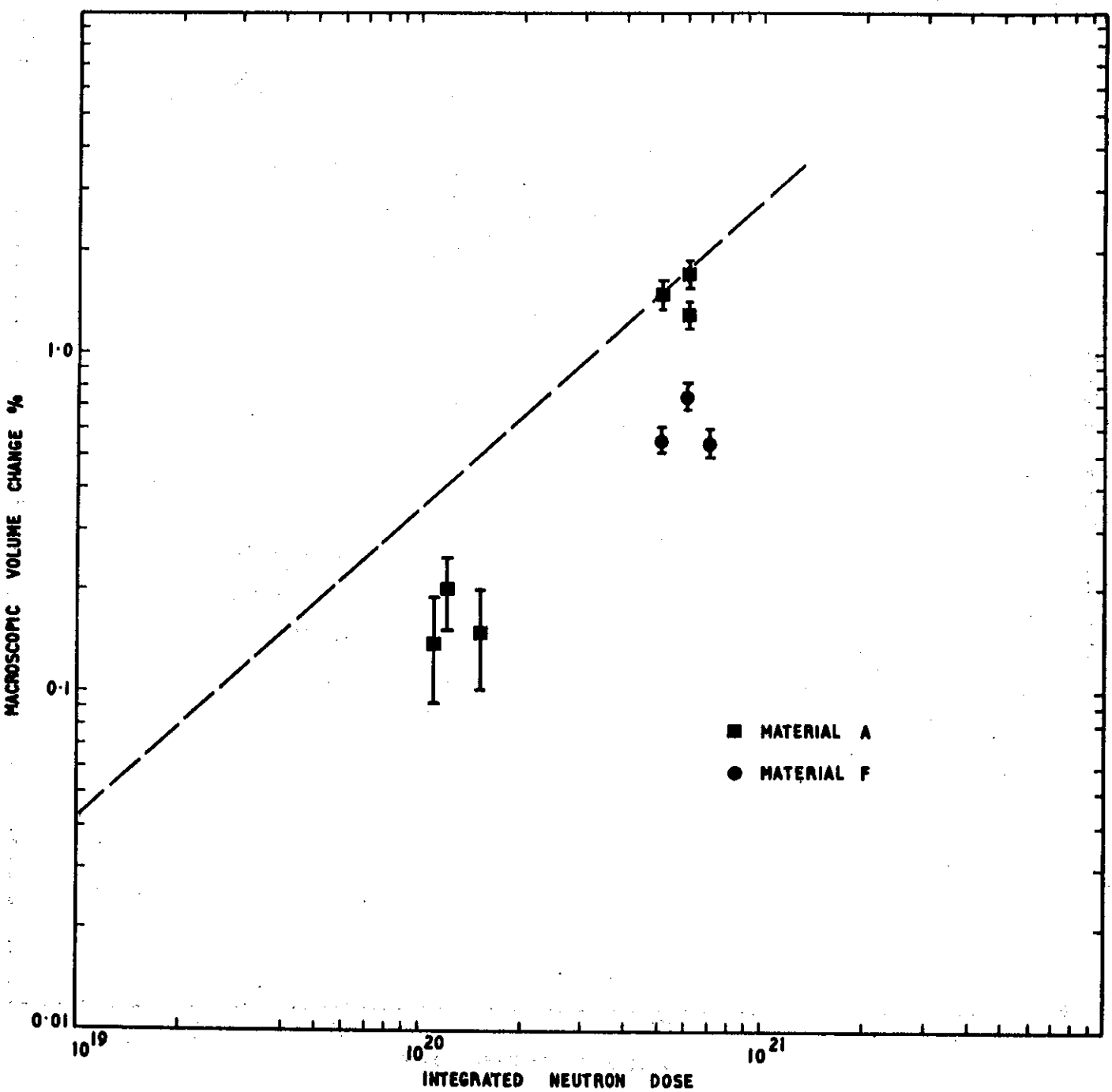

FIGURE 6.

MACROSCOPIC GROWTH VERSUS NEUTRON DOSE FOR MATERIAL IRRADIATED AT 500 - 700°C.

The broken line is taken from Figure 5 and represents the growth of coarse-grained material at < 100°C in the absence of crushing and crumbling.

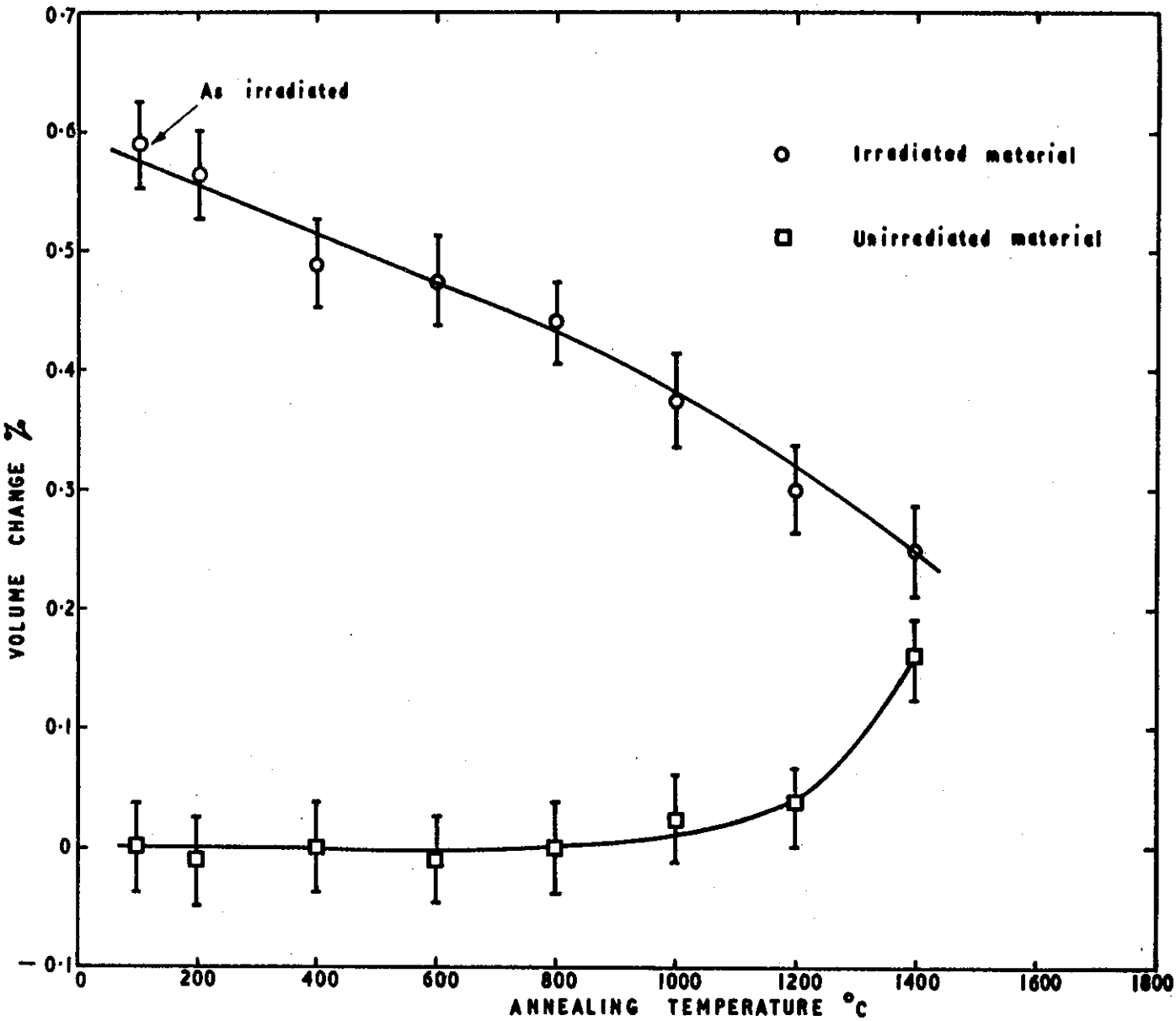

FIGURE 7. VOLUME CHANGES ON ANNEALING IRRADIATED AND UNIRRADIATED MATERIAL - (ONE HOUR ANNEALS)

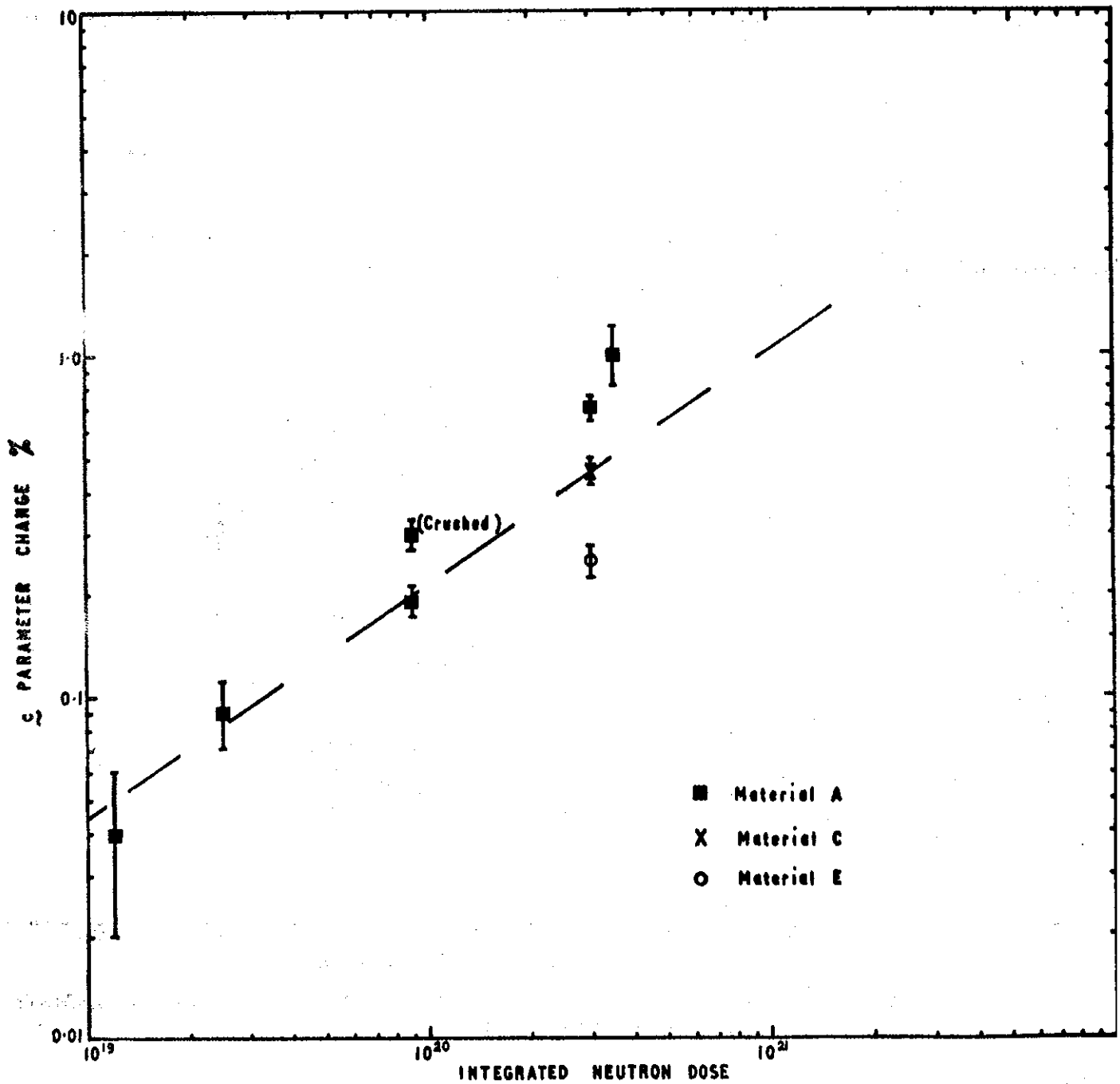

FIGURE 8. $\underset{\sim}{c}$ PARAMETER CHANGE VERSUS DOSE FOR IRRADIATION AT <100°C.
The broken line represents the growth of coarse-grained material in the absence of crumbling or crushing.

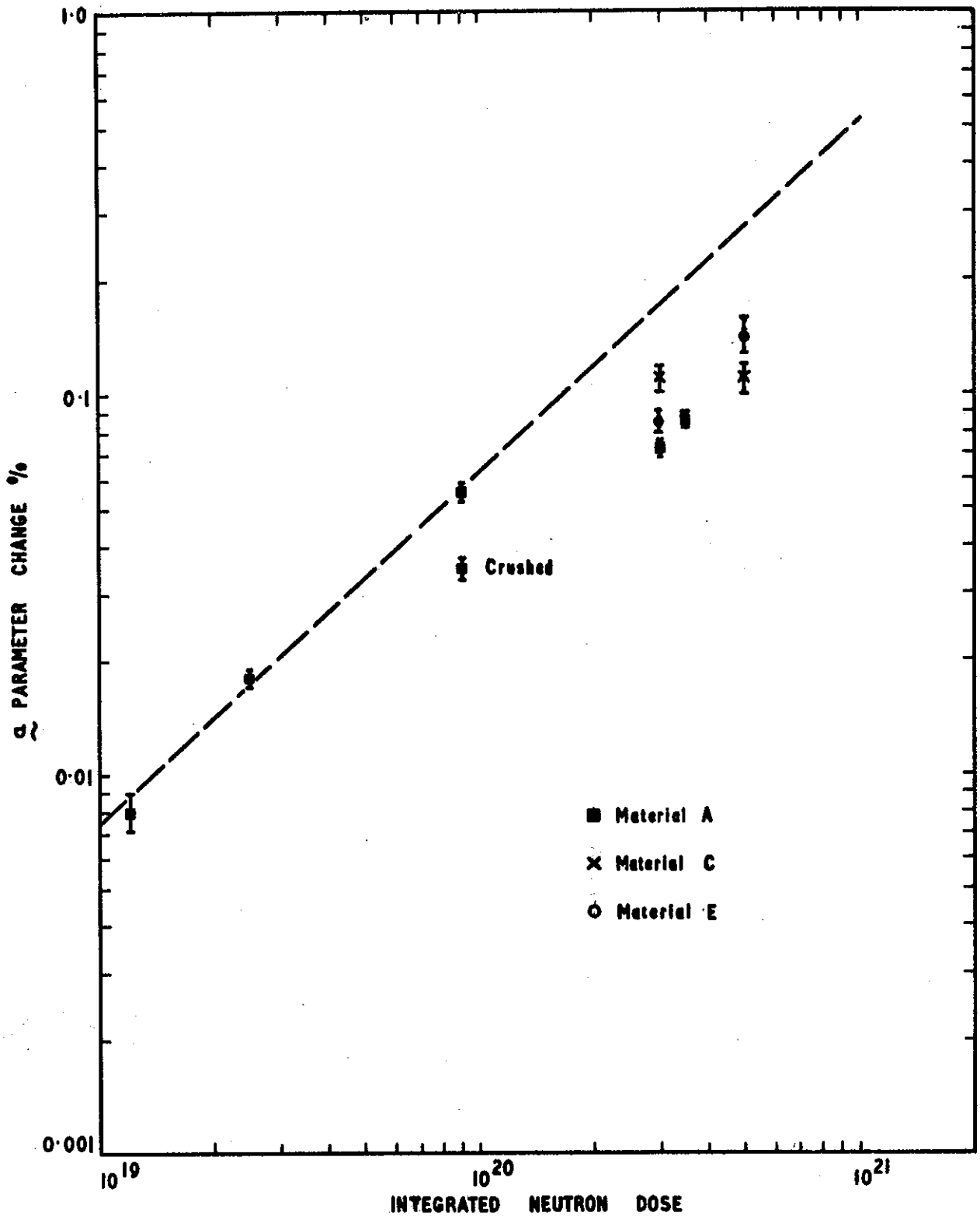

FIGURE 9.

α PARAMETER CHANGE VERSUS DOSE FOR IRRADIATION AT <100°C

The broken line represents the growth of coarse-grained material A in the absence of crumbling or crushing.

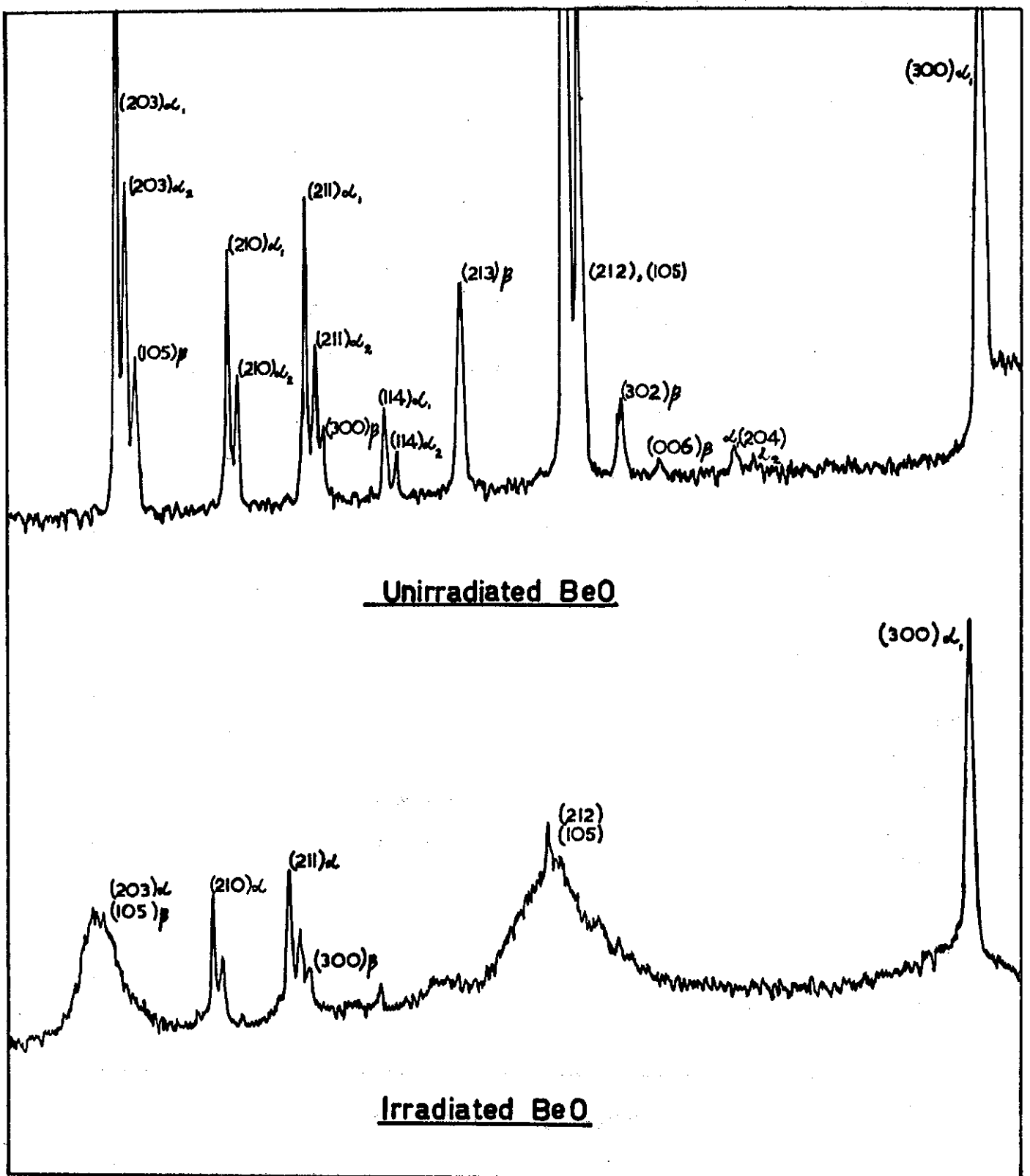

FIGURE 10 TRACING OF THE DIFFRACTOMETER CHARTS FOR UNIRRADIATED MATERIAL (TOP) AND FOR MATERIAL A IRRADIATED TO 3.5×10^{20} nvt AT $< 100\,^{\circ}C$.

This material had started to crumble under irradiation and the charts showed the extensive (h, k, l) line broadening when $l \neq 0$.

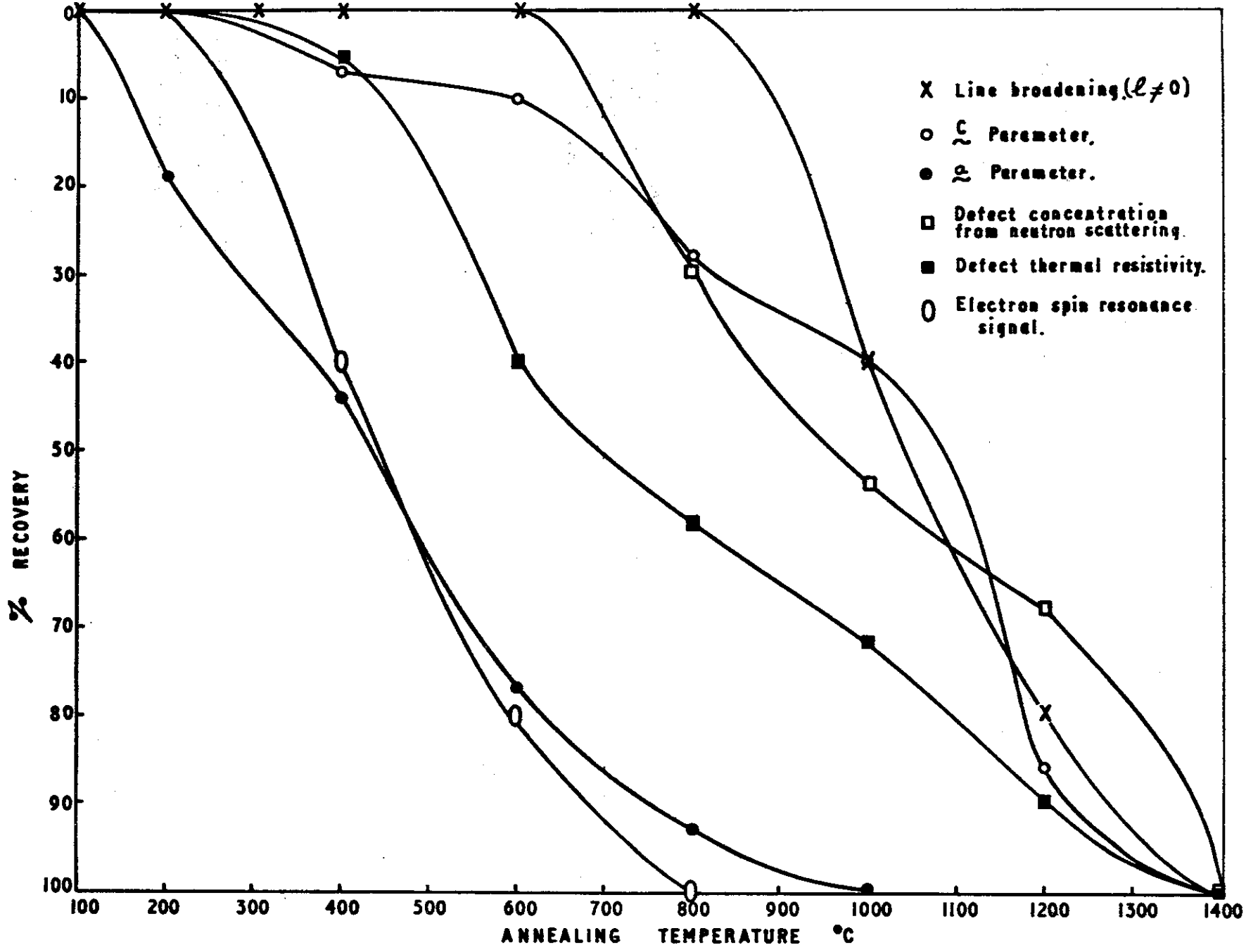

FIGURE II. ANNEALING OF VARIOUS PROPERTY CHANGES (ONE HOUR ANNEALS.)

X 500

(a) Unirradiated Material A showing sub–surface cracking. Polarized light.

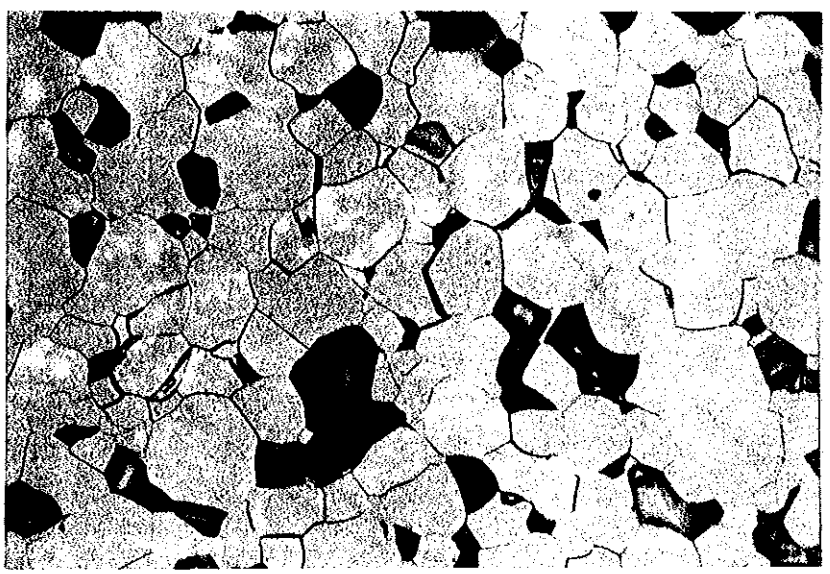

X 250

(b) Material B irradiated to 3×10^{20} nvt at $<100\,^{\circ}C$ showing extensive intergranular cracking and tear out of grains.

X 250

(c) Material C irradiated to 5×10^{20} nvt at $<100\,^{\circ}C$ showing some intergranular and transgranular cracking.

FIGURE 12 PHOTOMICROGRAPHS OF UNIRRADIATED AND IRRADIATED MATERIALS SHOWING MICROCRACKING

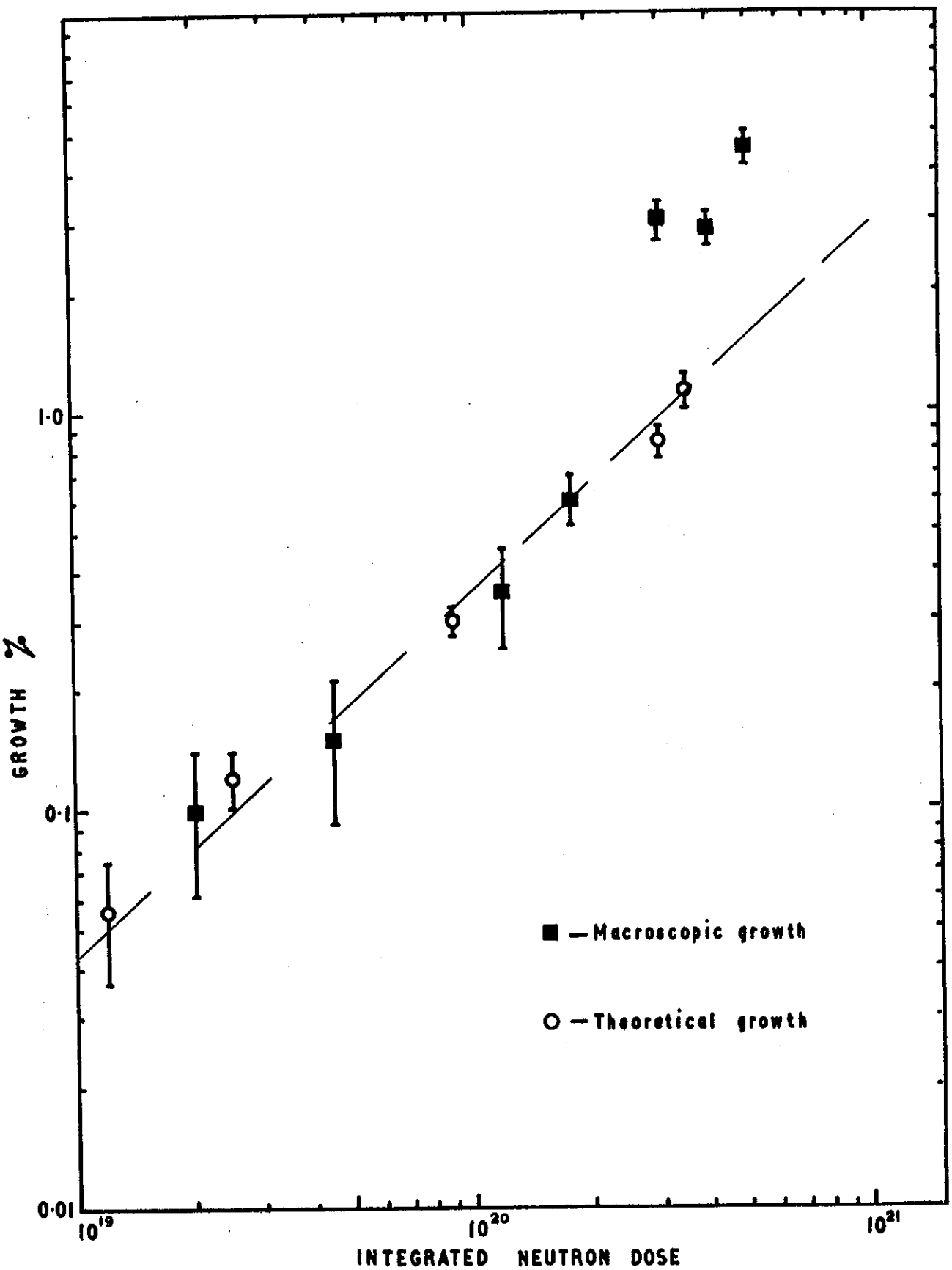

FIGURE 13. COMPARISON OF MACROSCOPIC GROWTH WITH THEORETICAL GROWTH AS CALCULATED FROM THE LATTICE PARAMETER CHANGES FOR MATERIAL A IRRADIATED AT $<100°C$.